The Astronomical Journal, 139:926–949, 2010 March doi:10.1088/0004-6256/139/3/926

PHOTOMETRIC STUDY OF THE KREUTZ COMETS OBSERVED BY *SOHO* FROM 1996 TO 2005

Matthew M. Knight[1,5,6], Michael F. A'Hearn[2], Douglas A. Biesecker[3], Guillaume Faury[4], Douglas P. Hamilton[2], Philippe Lamy[4], and Antoine Llebaria[4]

[1] Lowell Observatory, 1400 W. Mars Hill Road, Flagstaff, AZ 86001, USA; knight@lowell.edu
[2] Department of Astronomy, University of Maryland, College Park, MD 20742-2421, USA
[3] NOAA Space Weather Prediction Center, 325 Broadway, Boulder, CO 80305, USA
[4] Laboratoire d'Astronomie Spatiale, 38 Rue Frederic Joliot-Curie, 13388 Marseille Cedex 13, France
Received 2009 May 3; accepted 2010 January 6; published 2010 February 1

ABSTRACT

We present analysis of the photometry of more than 900 Kreutz comets observed by *SOHO* from 1996 to 2005. The Kreutz comets have "sungrazing" orbits with $q \approx 1$–$2\ R_\odot$, high inclinations ($i \approx 143°$), and periods of 500–1000 years. We find that they do not have a bimodal distance of peak brightness as previously reported, but instead peak from 10.5 $R_\odot$ to 14 $R_\odot$ (prior to perihelion), suggesting there is a continuum of compositions rather than two distinct subpopulations. The light curves have two rates of brightening, typically $\propto r^{-7.3\pm2.0}$ when first observed by *SOHO* (at distances of 30–35 $R_\odot$) then rapidly transitioning to $\propto r^{-3.8\pm0.7}$ between 20 $R_\odot$ and 30 $R_\odot$. It is unclear at what distance the steeper slope begins, but it likely does not extend much beyond the *SOHO* field of view. We derive nuclear sizes up to ∼50 m in radius for the *SOHO*-observed comets, with a cumulative size distribution of $N(>R) \propto R^{-2.2}$ for comets larger than 5 m in radius. This size distribution cannot explain the largest members of the family seen from the ground, suggesting that either the size distribution does not extend to the largest sizes or that the distribution is not uniform around the orbit. The total mass of the distribution up to the largest expected size (∼500 m) is $\sim 4 \times 10^{14}$ g, much less than the estimated masses of the largest ground-observed members. After correcting for the changing discovery circumstances, the flux of comets reaching perihelion has increased since 1996, and the increase is seen in comets of all sizes. Comparison of the *SOHO* comets with the *Solwind* and *Solar Maximum Mission* discoveries suggests there may have been an overabundance of bright comets arriving from 1979 to 1989, possibly indicative of a changing distribution around the Kreutz orbit.

Key words: comets: general – comets: individual (Kreutz Group) – methods: data analysis – techniques: photometric

1. INTRODUCTION

The Kreutz group of sungrazing comets contains some of the most spectacular comets on record, including the "Great Comet of 1882" (1882 II = 1882b = C/1882 R1) and Ikeya-Seki (1965 VIII = 1965f = C/1965 S1). The group was first recognized by Kirkwood (1880) and Kreutz (1888, 1891, 1901) on the basis of similar orbits of several comets from the 1600s and 1800s. As additional group members were observed in 1943, 1963, 1965, and 1970, Marsden (1967), Hasegawa (1966), Kresák (1966), Sekanina (1967a, 1967b), and others updated and expanded the analysis of the Kreutz group. Discovery of 16 fainter Kreutz comets from 1979 to 1989 (and three more in archival images since then) by the space-based coronagraphs *Solar Maximum Mission* (*SMM*) and *Solwind* (Sheeley et al. 1982; Michels et al. 1982; Weissman 1983; Marsden 1989; MacQueen & St. Cyr 1991), more than 1400 discovered by *SOHO* (Raymond et al. 1998; Uzzo et al. 2001; Biesecker et al. 2002), and a handful discovered by *STEREO* have renewed interest in the Kreutz group.

Much of this work has focused on the orbital dynamics of the largest members of the group. It has been well established that the two most prominent members, Ikeya-Seki and the Great Comet of 1882, split from each other very close to perihelion around the year 1100 CE (e.g., Marsden 1967; Sekanina & Chodas 2002a) and were quite possibly observed as the "Great Comet of 1106" (X/1106 C1). While the fragmentation history of the remaining ground-observed comets is not well understood, it is likely that they split from one or more parent fragments at some time prior to the 1500s, and that all of these parent fragments (including the parent of the Great Comet of 1882 and Ikeya-Seki) split from a single progenitor within the last 2500 years (Sekanina & Chodas 2002b, 2004, 2007, 2008). Sekanina & Chodas (2007) envision the Kreutz group to be much more populous than previously suggested, incorporating more than 20 poorly observed near-Sun comets recovered from the historical records by Hasegawa & Nakano (2001), Strom (2002), and England (2002), and potentially linking the progenitor with comets observed in 214 BCE, 423 CE, and/or 467 CE.

The *Solwind*-, *SMM*-, *SOHO*-, and *STEREO*-discovered comets are not sufficiently well observed to permit investigation of the dynamical history of individual comets. Instead, it has been demonstrated through statistical arguments (Sekanina 2000a, 2002a, 2002b) that these comets are likely products of runaway fragmentation throughout their orbits. In these models, the small coronagraphically discovered comets all split from their parent fragments since the previous perihelion passage. These fragmentation events occurred both before and after aphelion, at distances small and large. Splitting is likely to have continued in the newly produced fragments, with increasing time between subsequent events. Thus, the comets which are observed today are likely separated by several generations of fragmentation events from their source comet (the comet of which they were a part on the preceding perihelion passage). This widespread and repeated fragmentation results in a nearly steady stream of arrivals which have very different orbital elements and in most cases appear unrelated to each other.

[5] Work completed while at the University of Maryland.
[6] Author to whom any correspondence should be addressed.

Table 1
Properties of the Ground-observed Kreutz Comets

Comet	Radius (km)	Mass (g)	n	Range (AU)
1843 I = C/1843 D1 = Great March Comet	7.9	7.3×10^{17}	3.91	0.07–0.57
1880 I = 1880a = C/1880 C1 = Great Southern Comet	1.1	2.0×10^{15}	...	0.46
1882 II = 1882b = C/1882 R1 = Great Comet of 1882	30.7	4.2×10^{19}	3.51	0.58–4.42
1887 I = 1887a = C/1887 B1 = Great Southern Comet[a]	...	...	...	0.46,0.70
1945 VII = 1945g = C/1945 X1 = du Toit	0.6	3.9×10^{14}	...	(0.72)
1963 V = 1963e = C/1963 R1 = Pereyra	13.7	3.8×10^{18}	4.51	0.91–1.54
1965 VIII = 1965f = C/1965 S1 = Ikeya-Seki (pre)	4.3	1.2×10^{17}	(4.13)	(1.02–0.03)
(post)			3.90	0.04–1.63
1970 VI = 1970f = C/1970 K1 = White-Ortiz-Bolelli	1.1	2.1×10^{15}	3.21	0.26–0.90

Notes. Column (1) is the name of the comet. Columns (2) and (3) are the estimated nucleus radius and mass from the light curve parameters in Sekanina (2002a). Sizes were scaled assuming brightness is proportional to the square of the radius and a 4 m radius comet was magnitude 8 at 12 $R_\odot$. Mass was estimated assuming a bulk density of 0.35 g cm^{-3}. Columns (4) and (5) are the slope of the post-perihelion fading (pre-perihelion brightening) and range of heliocentric distances given by Sekanina (2002a). Pre-perihelion parameters are given in parentheses.

[a] No head or nuclear condensation was observed for C/1887 B1, so no size is estimated, and the rate of fading is poorly known.

As of 2009 October, there are more than 1400 known Kreutz comets. This includes eight that were seen from the ground (Table 1) and possibly another 20 or so if other poorly observed historical near-Sun comets are included, 19 that were seen with *SMM* and *Solwind*, 1431 that were discovered with *SOHO*, and 18 that were discovered with *STEREO*. The average elements of the *SOHO*- and *STEREO*-observed comets are $q = 0.0056 \pm 0.0013$ AU (note that $1\,R_\odot = 0.0046524$ AU, hence the term "sungrazing"), $\omega = 79\overset{\circ}{.}7 \pm 11\overset{\circ}{.}9$, $\Omega = 0\overset{\circ}{.}4 \pm 14\overset{\circ}{.}9$, and $i = 143\overset{\circ}{.}2 \pm 3\overset{\circ}{.}9$. Due to short orbital arcs, the eccentricity is indistinguishable from 1.0 for all but the brightest few members seen from the ground, making the periods of individual comets highly uncertain, but believed to be 500–1000 years. More than 90% of all Kreutz comets have orbits which resemble the "Subgroup I" orbit noted by Marsden (1967), while the remainder have orbits similar to "Subgroups II and IIa."

In this paper, we reduce and analyze photometry of the Kreutz comets observed by *SOHO* from 1996 to 2005. In Section 2, we discuss *SOHO*/LASCO. We summarize the reductions in Section 3. We present the light curves in Section 4, and interpret the photometry in Section 5. We discuss the population of the family based on the comets observed by *SOHO* in Section 6. Possible future observations are discussed in Section 7, and conclusions are given in Section 8.

2. OVERVIEW OF *SOHO*/LASCO

NASA's *SOHO* spacecraft was launched in 1995 December and began taking data in 1996 January. It is in a halo orbit around the Earth–Sun Lagrange point L1. *SOHO* contains a suite of instruments designed to continuously observe the Sun and the near-solar environment at varying wavelengths. By far the most prolific instrument for observing comets has been LASCO, which has discovered more than 1500 comets since 1996, and has observed other comets including 2P/Encke and 96P/Machholz 1 (Biesecker et al. 2002; Grynko et al. 2004; Lamy et al. 2003). Up to date lists of all comets discovered by LASCO can be found on the "Sungrazing Comets" Web site maintained by the U.S. Naval Research Laboratory.[7] This paper deals with the comets observed by LASCO, which is discussed in more detail below.

2.1. LASCO

LASCO contains three coronagraphs, C1, C2, and C3, which have nested fields of view ranging from 1.1 $R_\odot$ to 30 $R_\odot$ in the plane of the sky. The innermost coronagraph, C1, has an annular field of view ranging from 1.1 $R_\odot$ to 3.0 $R_\odot$. It is internally occulted, and has a narrow passband Fabry–Perot interferometer tuned to hot coronal emission lines (Brueckner et al. 1995). C1 was damaged in 1998 and has not been used regularly since. Telemetry since then has been re-allocated to the C2 and C3 coronagraphs. No comets have been seen in C1, nor was it designed to observe them. Therefore, it is omitted from further discussion.

The outer two coronagraphs, C2 and C3, have annular fields of view from 2.0 $R_\odot$ to 6.0 $R_\odot$ and 3.7 $R_\odot$ to 30 $R_\odot$, respectively. C2 was deliberately designed to overlap both C1 and C3. Both C2 and C3 are externally occulted broadband imaging telescopes. Each telescope has a filter wheel, a polarizer wheel, a shutter, and a 1024 × 1024 pixel CCD. The pixel scale is 11.9 arcsec pixel^{-1} for C2 and 56 arcsec pixel^{-1} for C3 (Brueckner et al. 1995).

The synoptic programs utilize approximately 85% of the available daily telemetry.[8] Originally, the white light synoptic program obtained one image each from C1 and C2 every 30 minutes, and an image from C3 every hour, with most images having a reduced field of view (most frequently 1024 × 768). However, since late 1998, typically three full-resolution C2 orange (5400–6400 Å) and two full-resolution C3 clear (4000–8500 Å) images are taken per hour. A polarization sequence using C2 and C3 is taken 1–2 times per day, and a color sequence is taken with C2 and C3 sporadically (sometimes as frequently as once per day, often as infrequently as once per week), usually at half-resolution (2 × 2 pixels binned so the full image is 512 × 512 pixels).

2.2. SOHO *Mission Interruptions*

SOHO has operated nearly continuously since launching in late 1995. It suffered a major interruption from 1998 June 24 until 1998 October 22, when it lost pointing and went into an uncontrolled spin. Smaller unplanned interruptions have occurred intermittently, such as a six week interruption from 1998 December until 1999 February. Pre-planned interruptions

[7] http://sungrazer.nrl.navy.mil/.

[8] http://lasco-www.nrl.navy.mil/index.php?=content/handbook/hndbk.

for routine maintenance, calibration, and satellite control have also occurred, and will continue to occur throughout the mission. Since the malfunction of the high-gain antenna in mid-2003, *SOHO* has needed to be rolled 180° every three months to keep the solar panels continuously pointing at the Sun. During these "keyhole" maneuvers which last approximately three weeks, some of the instruments are shut down. For a few days on either side of the roll maneuver, this frees up enough bandwidth and memory to increase the cadence of the C2 camera to five full-resolution images per hour.

3. REDUCTIONS

3.1. Calibrating Images

The *SOHO*/LASCO images we use for photometric reductions are "level-0.5" images which are publicly available via the *SOHO* Web site.[9] Level-0.5 images have been processed from the original data stream from the spacecraft ("level-0") into fits files and oriented so that solar north is at the top of the image. These images have units of DN (digital number or counts).

Reductions were done in IDL using many of the Solarsoft IDL routines.[10] Beginning with a level-0.5 image, we first subtract the offset bias. Next, we multiply the exposure time given in the FITS header by an exposure correction factor which is calculated for each image by the *SOHO* team (typically very close to 1.0), and divide the bias-subtracted image by the true length of exposure to convert it to a flux (DN s^{-1}). Then we multiply the bias-subtracted, normalized image by the vignetting function.[11] The vignetting in C3 changed slightly due to a shift in the optics during the mission interrupt in 1998. Therefore, three different vignetting functions are used when calibrating images: C2, C3 pre-interrupt, and C3 post-interrupt.

Median background images were constructed from four images, two prior to the image of interest, and two after the image of interest, each processed to DN s^{-1} as above. The images used in the background calculation are chosen to be as close in time to the image of interest as possible without contamination of the photometry aperture. Common contaminants are the comet itself (due to motion between images), background stars, cosmic rays, or blocks of data which were lost during downlinking from the spacecraft. We construct a background image using only images with the same telescope configuration (detector, filter, polarizer, summing on the chip, and telescope roll). Occasionally, fewer than four images are available for the background calculation, in which case the maximum number available is used. In general, images which were taken more than 24 hr apart are not used since transient solar activity causes the background levels to vary substantially over these timescales. We create the background image by taking the median value at each pixel. We then subtract the background image from the processed image of interest, yielding the final processed image. We have archived our processed images with the Planetary Data System (Knight 2008) where they are publicly available.

[9] http://sohowww.nascom.nasa.gov/data/realtime-images.html.

[10] Solarsoft is a data reduction and analysis package for solar physics, notably *SOHO*. It can be downloaded at http://sohowww.nascom.nasa.gov/solarsoft/.

[11] This corrects for the reduction in light received at the CCD due to the occulting disk and its support arm (the "pylon"). The optical transmission varies radially, from zero at the center (behind the occulting disk) to nearly 1 at the edges. Superposed on this, the "pylon" extends at a 45° angle from the southeast corner in unrolled images to the center.

3.2. Aperture Photometry

We calculated aperture photometry using a series of circular apertures centered on the optocenter of the comet. Aperture sizes were chosen to encompass the coma while minimizing contamination from background sources. For comparison across all comets, a circular aperture of radius 6 pixels (4.4 $arcmin^2$) was selected for C2 and 4 pixels (43.8 $arcmin^2$) for C3.[12] Aperture photometry of all of our processed images has been archived with the Planetary Data System (Knight 2009) and is publicly available.

Fluxes (DN s^{-1}) were converted to visual magnitude using zero-point conversions calculated by the *SOHO* team (A. Thernisien 2003, private communication; Llebaria et al. 2006). The zero points have changed slightly as the detector sensitivity has decreased over the life of the mission—by ∼0.4% per year in C3 and ∼0.7% per year in C2 (Thernisien et al. 2006; Llebaria et al. 2006). We use the global zero point calculated from 1996 to 2004 for C2 and from 1996 to 2003 for C3, and include an uncertainty due to the changing zero point of ±0.05 mag in the error estimate.

3.3. Normalization of the Magnitude

Since the focus of our study of the light curves is to derive the dependence of the brightness on the heliocentric distance, the apparent magnitude is corrected for Δ (the comet–spacecraft distance) and phase angle (the Sun–comet–spacecraft angle, θ), but not for r (the Sun–comet distance). Comet fluxes are normalized to $\Delta = 1$ AU, although we assume that *SOHO* is always at L1 (the Lagrange point along the Sun–Earth line) and do not correct for the minor deviations from L1 caused by its orbit. These deviations are less than 1% of the comet–spacecraft distance and have been ignored because their effect on the magnitude is much less than the uncertainty from the photometric reductions (discussed in the following section).

The correction for phase angle is much less straightforward and has a much larger effect on the interpretations of the light curves. Due to their highly eccentric orbits, small perihelion distances, and high velocities, Kreutz comets observed close to perihelion can undergo dramatic changes in phase angle over very short timescales (up to 50° in ∼2 days). Furthermore, many are seen at large phase angles, some in excess of 150°. Only a few non-sungrazing comets have been observed at such large phase angles. These include 1P/Halley, Skjellerup-Maristany (1927 IX = 1927k = C/1927 X1), West (1975 VI = 1975n = C/1975 V1), Bradfield (1980 XV = 1980t = C/1980 Y1), 96P/Machholz 1 (in 2002), C/2004 F4 (Bradfield), and C/2006 P1 (McNaught), all of which showed large increases in brightness (Ney & Merrill 1976; Ney 1982; Marcus & Seargent 1986; Gehrz & Ney 1992; Grynko et al. 2004; Marcus 2007b, 2007c). Thus, it is necessary to correct the apparent magnitudes for the changing phase angle before attempting to understand the heliocentric brightness dependence.

Kolokolova et al. (2004) combined observations of a number of comets over a wide range of phase angles and produced a plot (their Figure 1) for the phase dependence of cometary albedo due to scattering off dust in the coma. This shows a strong forward-scattering (scattering in roughly the same direction that photons were traveling) surge at phase angles greater than 100°, a relatively flat region at intermediate phase angles, and

[12] These radii are for full-resolution 1024 × 1024 images. Half-resolution 512 × 512 images use apertures with half the radius.

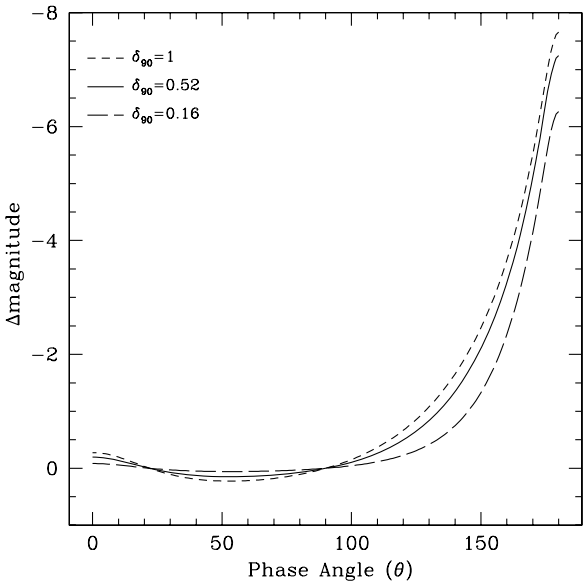

Figure 1. Marcus (2007b) phase function as given by Equation (1). Three dust-to-gas light ratios (δ_{90}) are plotted: 1 (dashed line), 0.52 (solid line), and 0.16 (long-dashed line).

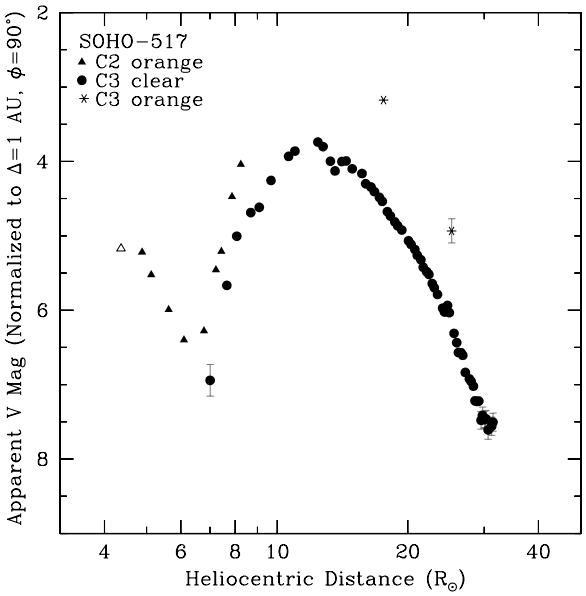

Figure 2. Light curve of C/2002 S2 (*SOHO*-517) which is representative of the typical Kreutz light curve shape. The triangles are C2 orange filter images, circles are C3 clear filter images, and asterisks are C3 orange filter images. The open points are images which had vignetting greater than 4.0. Error bars smaller than 0.1 mag (for the upper error bar) have been suppressed.

a slight back-scattering (scattering opposite the initial direction of motion of the photons) peak at phase angles smaller than 30°.

Marcus (2007b) examined the phase dependence of coma brightness due to dust, deriving a "compound Henyey–Greenstein" (HG) model of the phase function which combines separate HG functions for forward- and back-scattering. Similar in shape to the Kolokolova et al. (2004) figure, this model can be adjusted for varying coma dust-to-gas light ratios, and accurately predicted the surge in brightness of C/2006 P1 (McNaught) at large phase angle (Marcus 2007a, 2007c). The full form of the compound HG model is given in Equation (1) of Marcus (2007c)

$$\phi(\theta) = \frac{\delta_{90}}{1+\delta_{90}}\left[k\left(\frac{1+g_f^2}{1+g_f^2-2g_f\cos(180-\theta)}\right)^{\frac{3}{2}} + (1-k)\left(\frac{1+g_b^2}{1+g_b^2-2g_b\cos(180-\theta)}\right)^{\frac{3}{2}} + \frac{1}{\delta_{90}}\right], \quad (1)$$

where $\phi(\theta)$ is the scattering function which can be converted to a magnitude by $\Phi(\theta) = 2.5\log[\phi(\theta)]$, θ is the phase angle, δ_{90} is the dust-to-gas light ratio of the coma at $\theta = 90°$, k is the partitioning coefficient between forward- and back-scattering ($0 \leqslant k \leqslant 1$), and g_f and g_b are the forward- and back-scattering asymmetry factors ($0 \leqslant g_f < 1$ and $-1 < g_b \leqslant 0$). Marcus (2007b) fit the data using $g_f = 0.9$, $g_b = -0.6$, $k = 0.95$, and $\delta_{90} = 1$ for an "usual" comet or $\delta_{90} = 10$ for a "dusty" comet. The function $\Phi(\theta)$ is normalized to 0 mag correction at a phase angle of 90°, and is plotted in Figure 1.

As will be discussed in Section 4.3, Kreutz comets appear ∼1 mag brighter in the orange than in the clear filter, which is attributed to sodium emission. The contribution of the sodium emission to the flux must therefore be accounted for to properly apply the scattering correction. In Section 5, we estimate the flux of sodium emission necessary to cause the comets to appear ∼1 mag brighter in the orange than in the clear filter. The ratio of the flux due to the solar continuum (scattering off the dust in the coma) to the flux due to the sodium emission (gas) is $\delta_{90} = 0.52$ for the C3 clear filter and $\delta_{90} = 0.16$ for the C2 orange and C3 orange filters. These values of δ_{90} result in a smaller correction due to phase angle than was found by Marcus (2007b) for typical comets, but are necessary to account for the strong contribution of sodium to the apparent brightness of the Kreutz comets. The other parameters were left unchanged, as they proved robust for the sample of six comets fit by Marcus (2007b, 2007c). With these parameters, we use Equation (1) to correct the apparent visual magnitude to a phase angle of 90°.

3.4. Estimating the Error

The total error (in magnitudes) is a combination of the errors from the various components which went into the magnitude calculation added in quadrature. These include uncertainty in the counts (calculated using counting statistics for the electrons received on the CCD), heliocentric distance (assumed to be 1%), phase angle (estimated to be 10% of the magnitude correction), and the zero-point scale (estimated to be ∼0.05 mag to account for the decreasing sensitivity of the detectors). Other sources of uncertainty were ignored because they were much smaller than the above estimated errors. These include the bias, dark count, exposure time, vignetting function, and several other characteristics of the CCD and telescope optics which are discussed by Morrill et al. (2006).

4. LIGHT CURVES

Prior to *SOHO*, most Kreutz comets had only been seen after perihelion (most ground-observed comets) or inside of ∼15 $R_\odot$ (the *SMM* and *Solwind* comets). A surprising trait of the Kreutz comets observed by *SOHO* is the shape of their light curves, illustrated in Figure 2, and first discussed in Biesecker et al. (2002). Typical Kreutz comets brighten steadily as they approach the Sun, begin to flatten out at ∼16 $R_\odot$, reach a peak in brightness prior to perihelion at a distance of 10–14 $R_\odot$, then fade as they continue to approach the Sun. Occasionally, the fading flattens out or they brighten again at distances inside of ∼8 $R_\odot$ before disappearing. No Kreutz comet observed by *SOHO* has ever been seen after perihelion. Due to seasonal

Table 2
Comets that Peak in C3, Listed in Order of Peak Distance

Designation	*SOHO*	Distance of Peak ($R_\odot$)	C2 Peak Magnitude	C3 Peak Magnitude	Universal Curve	Group
C/1998 A1	37	9.1–13.6	...	6.6	1	...
C/2000 H2	*111*	*9.7*	*0.5*	*0.7*	...	...
C/1996 O2	22	10.0–14.5	...	6.1	1	...
C/1996 O4	23	10.1–12.8	...	5.4	1	...
C/1997 R3	29	10.1–12.3	<7.4	6.6	1	...
C/1997 L3	12	10.6	...	5.0	2	C
C/2002 J3	443	10.7	<2.9	4.1	...	C
C/1998 K10	*54*	*10.8*	*0.6*	*0.8*	...	...
C/2001 C6	296	10.8	<5.6	5.3	...	C
C/2003 K7	*614*	*10.8*	*−0.0*	*−0.1*	...	...
C/2005 F1	925	10.8	<6.2	6.2	...	B
C/1998 K11	*55*	*10.9*	*0.1*	*0.5*	...	...
C/1997 T2	31	10.9	<5.6	6.4	2	C
C/1997 L4	13	11.0–12.0	3.5	4.5	1	...
C/1997 M1	15	11.1	...	5.7	2	C
C/2000 C6	104	11.1	...	5.2	...	C
C/2003 O5	644	11.1	<5.0	4.2	...	C
C/2005 L7	972	11.1	3.3	4.3	...	B
C/2000 D1	106	11.2	...	5.1	...	C
C/2006 B3	1091	11.2	...	6.2	...	A
C/2006 B6	1094	11.2	...	5.8	...	C
C/1997 S1	30	11.3–14.3	<6.8	7.5	1	...
C/2000 B6	98	11.3	...	6.3	...	C
C/2005 C3	907	11.3	...	5.0	...	B
C/2005 E6	917	11.3	<5.9	5.3	...	C
C/1998 G4	47	11.4	<3.8	4.6	2	C
C/1996 Q3	2	11.5	...	6.4	2	C
C/2003 Q7	657	11.5	...	4.5	...	C
C/2004 T7	844	11.5	<5.5	6.9	...	B
C/2001 C3	293	11.6	...	5.9	...	A
C/1999 O3	74	11.7	...	5.7	...	C
C/2006 A5	1087	11.7	<3.7	3.9	...	A
C/1997 K1	10	11.8–13.0	3.9	4.9	1	...
C/2003 A3	579	11.8	...	5.4	...	A
C/2004 O1	819	11.8	...	4.8	...	B
C/2004 Q4	830	11.8	...	6.1	...	B
C/2003 Q5	655	11.9	...	4.9	...	C
C/2003 V5	687	12.0	<4.8	5.9	...	A
C/2003 W6	694	12.0	<4.4	6.0	...	A
C/2004 A2	724	12.0	...	4.7	...	B
C/2004 Q3	829	12.0	...	6.3	...	B
C/2001 C2	294	12.1	...	4.2	...	A
C/2003 C5	587	12.1	...	6.4	...	B
C/2000 E1	107	12.2	...	5.3	...	A
C/2004 P7	828	12.2	...	5.8	...	B
C/2005 D5	913	12.2	<6.4	5.5	...	A
C/2005 P1	999	12.2	...	6.5	...	A
C/2005 V9	1047	12.2	<4.0	4.9	...	A
C/2005 Y9	1078	12.2	<4.9	6.3	...	A
C/1996 H1	17	12.3–13.7	...	4.7	2	...
C/1996 O4	23	12.3	...	5.4	...	C
C/2000 B1	97	12.3	...	4.3	...	A
C/2002 Q7	503	12.3	...	5.6	...	B
C/2003 C2	584	12.3	...	4.0	...	A
C/2003 Q2	652	12.3	...	5.2	...	A
C/2004 F6	750	12.3	<5.0	5.3	...	A
C/2005 O3	995	12.3	<6.2	4.5	...	A
C/2002 S2	517	12.4	<4.0	3.7	...	B
C/2002 W12	556	12.5	<4.8	6.4	...	A
C/1999 C1	58	12.5	...	5.4	...	A
C/1997 P1	19	12.6	...	3.3	1	A
C/1999 S1	86	12.6	...	4.8	...	A
C/2003 F5	594	12.6	<3.0	3.8	...	A
C/2005 N9	993	12.6	<5.5	5.2	...	B
C/2004 R4	833	12.7	...	5.8	...	B
C/1997 Q2	25	12.8	...	4.3	1	A
C/1998 L1	56	12.8	<5.5	5.4	1	B
C/2001 R2	*347*	*12.8*	*<3.8*	*2.9*	...	...
C/2003 F3	592	12.8	<4.2	4.4	...	C
C/2000 T1	204	12.9	<3.4	4.3	...	A
C/2003 L5	624	12.9	3.0	4.0	...	B
C/2004 D4	744	12.9	...	4.5	...	A
C/1996 S3	3	13.0	...	5.5	1	A
C/1998 H2	48	13.0	<1.1	2.1	...	A
C/2001 U9	*367*	*13.1*	*<1.4*	*2.8*	...	...
C/2005 T11	1031	13.2	<5.3	5.8	...	A
C/2001 U4	361	13.7	<6.3	7.3	...	A
C/2005 S1	1024	13.7	<3.8	4.1	...	A
C/2001 U7	365	14.0	<4.3	5.5	...	A

Notes. Column (1) is the IAU designation. Column (2) is the internal *SOHO* number. Column (3) is the heliocentric distance of peak brightness. The comets for which a range of distances are given were included in Biesecker et al. (2002) but we could not determine the peak. Column (4) is the apparent visual magnitude of the peak in C2. When the peak was not visible, the maximum observed brightness in C2 is listed along with a "<" symbol. Column (5) is the apparent visual magnitude of the peak in C3. Column (6) denotes membership in "universal curve" 1 or 2 from Biesecker et al. (2002). Column (7) denotes the group in which we have classified the shape of the light curve. The comets which are italicized saturated the detector and were therefore excluded from the group analysis.

geometric effects, data gaps, and/or the sensitivity of the detectors, most comets are not observed well enough to exhibit all of these features. However, nearly every comet displays some component of this general shape, and none are in contradiction to it.

In this section, we discuss the light curves of the 924 comets that reached perihelion from 1996 January to 2006 January for which we have calculated photometry. The photometry was calculated as described in Section 3, and has been normalized to unit *SOHO*-centric distance and corrected to a phase angle of 90° unless otherwise noted.

4.1. Peak Distance

Biesecker et al. (2002) studied the first 141 Kreutz comets observed by *SOHO* from 1996 to 1998. Of these, 17 were determined to reach a peak brightness in C3 without saturating the detector (the peaks are not well observed in C2 due to its limited field of view and so C2 data were excluded). The peak distances of these 17 were found to be bimodal, with 11 comets in their Universal Curve 1 (UC1) reaching peak brightness at a slightly larger heliocentric distance (12.3 $R_\odot$) than the remaining six in Universal Curve 2 (UC2), which peaked at 12.3 $R_\odot$. Furthermore, UC2 brightened and faded more rapidly than did UC1. With our much larger sample size, we are equipped to more rigorously test the bimodality of peak distance and the existence of the universal curves.

We were able to determine a peak in the light curve in C3 for 65 comets. Peaks were determined by a combination of fitting a quadratic to the data and by selecting the single brightest photometric values. It is difficult to determine the exact peak distance of most light curves as they often have a broad, flat peak over a distance of 1–2 $R_\odot$. Thus, we estimate the uncertainty in peak distance could be as large as ±0.5 $R_\odot$. Table 2 lists these 65 comets, six additional comets which peaked in C3 but saturated

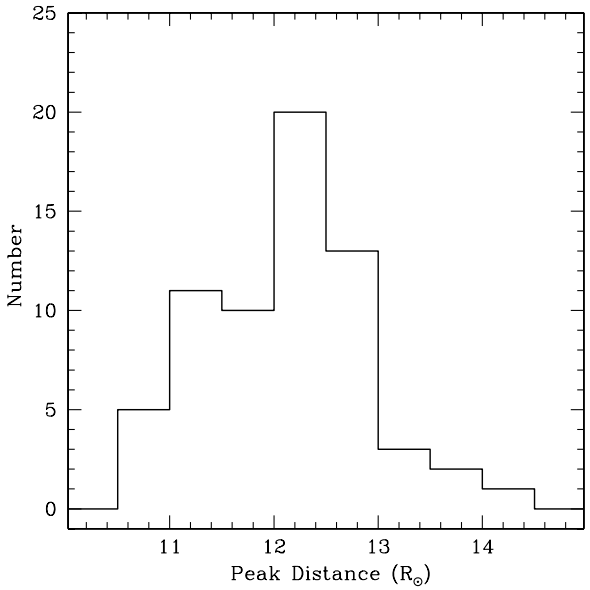

Figure 3. Histogram of the heliocentric distance of peak brightness for comets observed to peak in C3.

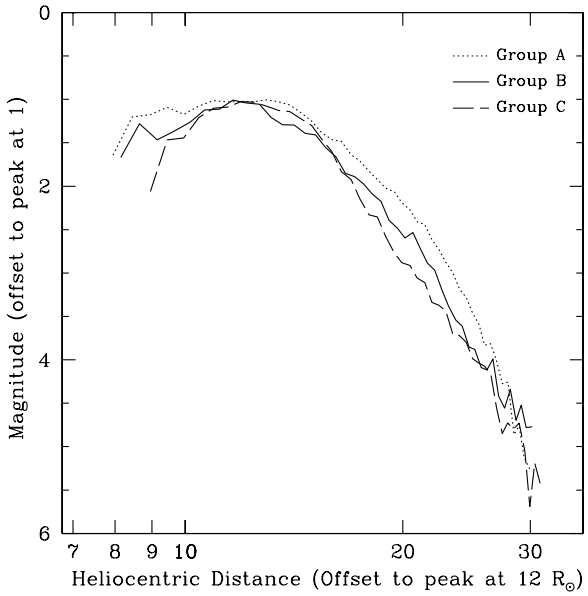

Figure 4. Plots of the three groups normalized so that they all peak at a magnitude of 1 and a heliocentric distance of 12 $R_\odot$. A is the dotted line, B is the solid line, and C is the dashed line.

the detector, and eight comets from Biesecker et al. (2002) for which we could not reliably determine a peak because the data were too sparse near the peak (the remaining nine comets from Biesecker et al. 2002 were in our original 65).

A histogram of the heliocentric distance of peak brightness for the comets observed to peak in C3 is shown in Figure 3. The histogram has a maximum at 12.0–12.5 $R_\odot$ and a shoulder at 11.0–11.5 $R_\odot$. These features are consistent with the bimodality seen by Biesecker et al. (2002). However, unlike the Biesecker et al. (2002) sample, we also find a broad range of peak distances from 10.5 $R_\odot$ to 14 $R_\odot$. Thus, while the sample retains the preference for peaking in brightness near 11 $R_\odot$ or 12 $R_\odot$, there is a continuum of peak distances centered around 12 $R_\odot$. Inclusion of the eight comets from Biesecker et al. (2002) for which we could not determine a peak distance does not affect the conclusion of a continuum of peak distances. If these eight are removed from the Biesecker et al. (2002) sample, the remaining nine comets show an even larger bimodality of peak heliocentric distance: 12.8 $R_\odot$ for UC1 and 11.2 $R_\odot$ for UC2.

The geometry of the orbit makes it rare to see Kreutz comets at heliocentric distances smaller than 10 $R_\odot$ in C3. While the C3 field of view extends to 3.7 $R_\odot$ in the plane of the sky, the photometry becomes increasingly unreliable at small distances, as the vignetting and sky background increase and transient solar activity becomes more common. In principle, comets should be observable until well after their peak in C3, but some peaks are probably not recognized as a result. This is more likely to occur for fainter comets and those that peak at smaller heliocentric distances.

We investigated whether the universal curves were evident in our larger sample. Rather than looking strictly at the distance of peak brightness, we considered the shape of each comet's light curve, which appears to be correlated with the distance of peak brightness as discussed by Biesecker et al. (2002). To further examine the possible correlation, we put the individual light curves in one of three groups based on their shape. The choice of three groups is somewhat arbitrary, as four or five groups could have been identified, but the number of comets in each group would become problematic for statistics. To avoid confusion with the nomenclature of Biesecker et al. (2002), we designate these groups A–C from largest peak distance to smallest. Column (7) of Table 2 lists the group of each of the comets observed to peak in C3.

We constructed composite curves for each group by offsetting all the comets in a given group to peak at the same magnitude and taking the median magnitude of all the observations in a given heliocentric distance range (Figure 4). Group A is similar to UC1. It contains 31 comets with a median peak distance of 12.3 $R_\odot$. Group B contains 16 comets with a median distance of 12.1 $R_\odot$. Group C is similar to UC2, containing 18 comets with a median peak distance of 11.3 $R_\odot$. C brightens most steeply while A has the shallowest slope of brightening. At distances larger than ~24 $R_\odot$, all three groups have similar slopes. The slopes of fading are harder to distinguish than the brightening due to fewer observations over a smaller region and generally noisier data. However, C fades the most rapidly, followed by B, with A fading the most gradually.

We searched for trends that might correlate with the characteristic shape of these groups. There were no trends with orbital elements (q, Ω, ω, or i). Furthermore, there are members of all three groups in both of Marsden (1967)'s "Subgroups I and II," suggesting that the light curve behavior is not dependent on the major fragment from which each comet is descended. The groups do not show a seasonal dependence. The mean and median peak magnitudes are similar, and similar percentages of each group are brighter than magnitude 5 or 6. Therefore, it does not appear that there is a difference in internal strength between the groups which might affect the propensity for fragmentation and thus the size distribution of the groups.

Interestingly, 15 of the 16 comets in group B have been discovered since mid-2002. Prior to 2003, nearly all the comets observed to peak in C3 were members of groups A or C. However, since then all but five comets have been in groups A or B. This may be diagnostic of a varying composition of the swarm of Kreutz comets as a function of true anomaly in the orbit. That is, there may be some clustering of composition on the timescale of years, and the comets with compositions causing them to brighten as group B only began reaching perihelion en masse in

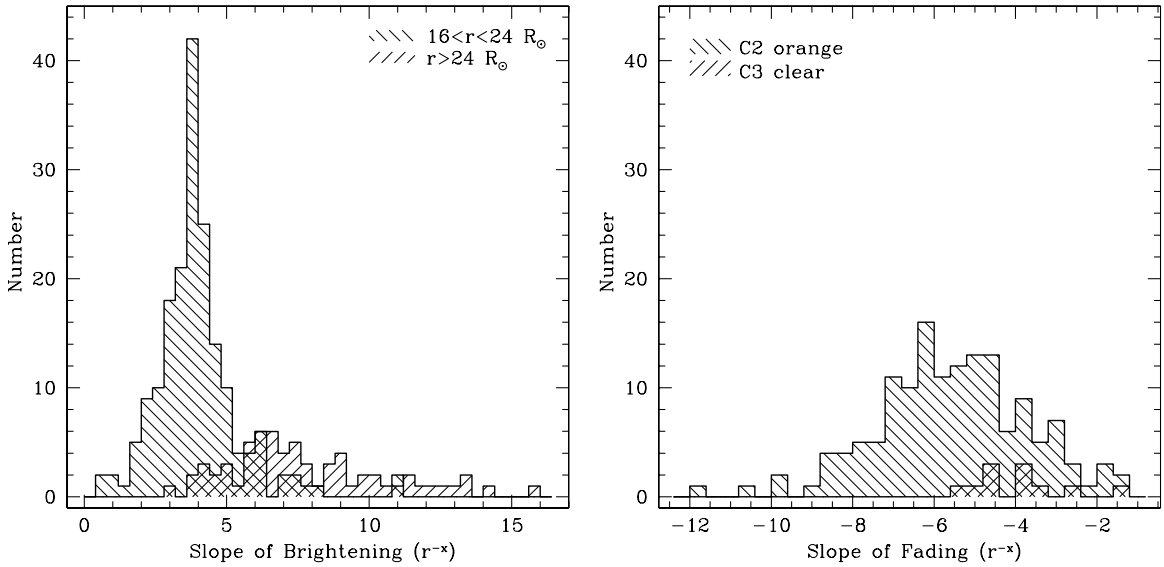

Figure 5. Histograms of the slope of the brightening (left panel) and fading (right panel) of Kreutz comets. The slopes of brightening are calculated for two regions in the C3 clear filter: distances larger than 24 $R_\odot$ (hatching at +45°) and from 24 to 16 $R_\odot$ (hatching at −45°). The slopes of fading are calculated from 10 to 7 $R_\odot$ for the C3 clear filter (hatching at +45°) and the C2 orange filter (hatching at −45°). All distances are prior to perihelion.

2003. This would explain the apparent decrease in frequency of comets peaking near 11.2 $R_\odot$ since 1996–1998 (Biesecker et al. 2002's sample).

An alternative explanation is that the increase in group B comets is a result of improved detection circumstances for *SOHO*. As will be discussed in Section 6.2, there have been numerous changes to the way in which *SOHO* observes since 2000. These changes make it more likely that comets will be well observed and thus easier to identify the peak in the light curve, the criteria for being included in this study. It is possible that the flux of group B comets has remained constant throughout the mission, but our ability to recognize them as such has improved. However, if this were the case we would expect group C, which peaks more sharply than group B, to also show an increase since its peak should also be better observed. In fact, there has been a decrease in group C comets, and we conclude that there is some evidence suggesting compositional differences along the Kreutz orbit.

4.2. Brightening and Fading

While there are a limited number of comets for which the distance of turnover can be determined, there are many partial light curves available to give information about the brightening and fading behavior. We considered slopes (slope $= x$, where brightness $\sim r^{-x}$) over three ranges: brightening at heliocentric distances larger than 24 $R_\odot$, brightening from 24 $R_\odot$ to 16 $R_\odot$, and fading from 10 $R_\odot$ to 7 $R_\odot$. We considered two regions for the brightening slope because there appears to be a break in the slope for many comets between 20 $R_\odot$ and 27 $R_\odot$. We calculated fading slopes for both C2 orange and C3 clear images. However, we only calculated brightening slopes for C3 clear images as no comets were observed in C2 beyond 16 $R_\odot$, and very few comets were observed well enough in C3 orange images to calculate a slope. We did not calculate any slopes from 10 $R_\odot$ to 16 $R_\odot$ because this is the region where light curves turn over. We also did not calculate any slopes at distances smaller than 7 $R_\odot$ because the light curves tend to be chaotic at these distances. All comets with at least five images within the specified ranges that could be reasonably well fit by a power law were used. This frequently excluded the faintest comets (typically fainter than magnitude ∼7), where the uncertainty in the magnitude was comparable to the extent of the brightening or fading. Histograms of the brightening (left panel) and fading (right panel) are plotted in Figure 5. Table 3 summarizes the median slopes in each distance range. Note that the median slope of brightening from 24 $R_\odot$ to 16 $R_\odot$ is 3.8, which is very close to the canonical r^{-4} dependence of comet brightening. This will be explored more in Section 5.

The change in the slope of brightening that occurs around 24 $R_\odot$ is striking. While there is significant spread in the slopes beyond 24 $R_\odot$, the slope is unmistakably steeper than the slope from 24 $R_\odot$ to 16 $R_\odot$. The spread in slopes beyond 24 $R_\odot$ is likely due to fewer images, higher noise, and the distance of the break in the slope varying from comet to comet and not always occurring at 24 $R_\odot$. It is unlikely that the steeper slope is a product of poor photometry caused by faint comets because there are comparable numbers of equally faint observations in the 24–16 $R_\odot$ range without a corresponding tail of steep slopes. Assuming the change in slope is real, it may be tied to an ongoing physical process which is typically exhausted around 24 $R_\odot$. We will consider possible scenarios in Section 5.

4.3. Orange–Clear Magnitude Difference

While the shapes of the light curves in the orange and clear filters tend to be similar, the comets generally appear brighter in the C2 and C3 orange filters than in the C3 clear filter. If the comet brightness was due entirely to reflected solar continuum, the magnitudes would be the same in both the orange (5400–6400 Å) and clear (4000–8500 Å) filters. However, comet brightness is also due to emission, and so the fractional increase in light due to emission has a larger effect in a narrower bandpass than in a wider bandpass. For emission between 5400 Å and 6400 Å, the comet will appear brighter in the 1000 Å wide orange filter than in the 4500 Å wide clear filter.

There are relatively few overlapping orange and clear observations because comets are rarely observed simultaneously in C2 and C3, and because C3 orange images are taken infrequently. Furthermore, those that do overlap tend to be noisy due

Table 3
Median Light Curve Parameters

Parameter	No.	Corrected Data (Median ± SIQR[a])	Raw Data (Median ± SIQR)
Peak distance ($R_\odot$)	65	12.2 ± 0.55	11.9 ± 0.45
Slope of C2 orange fading from 10 to 7 $R_\odot$	145	−5.5 ± 1.2	−5.1 ± 0.9
Slope of C3 clear fading from 10 to 7 $R_\odot$	11	−3.9 ± 0.7	−3.9 ± 0.9
Slope of C3 clear brightening from 24 to 16 $R_\odot$	181	+3.8 ± 0.7	+3.9 ± 0.6
Slope of C3 clear brightening beyond 24 $R_\odot$	67	+7.3 ± 2.0	+8.0 ± 1.9
Slope of size distribution	219	−2.22	−2.22
Median orange–clear magnitude difference	126	−1.19 ± 0.34	−1.03 ± 0.30

Notes. Column (1) lists the parameters. Column (2) lists the number of comets used to calculate the parameters. Column (3) lists the values used in this paper. Column (4) lists the values which would be derived if the data were not normalized to a unit *SOHO*-centric distance and corrected for phase angle.
[a] SIQR (semi-interquartile range) is a measure of volatility. It is half the distance between the 25th and 75th percentiles.

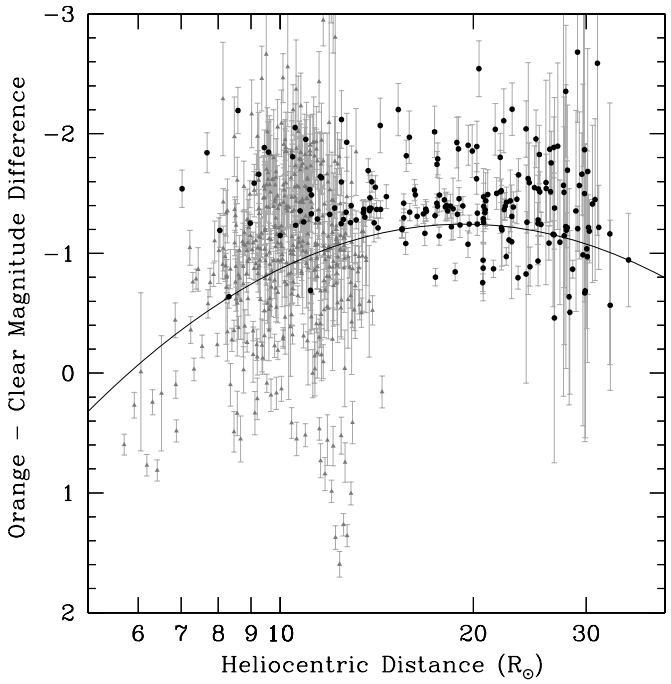

Figure 6. Orange–clear magnitude difference as a function of heliocentric distance. Negative values are brighter in the orange than the clear. The black circles are C3 orange–C3 clear magnitudes and the gray triangles are C2 orange–C3 clear magnitudes. The line is the best-fit quadratic to the data, which peaks at 18.6 $R_\odot$.

to the proximity to the C3 occulter for comets observed simultaneously in C2 and C3. Only a handful of comets have more than three overlapping orange and clear images, making it difficult to draw conclusions from the color behavior of individual comets. Instead, we consider the orange–clear magnitude difference in the aggregate.

Figure 6 shows the orange–clear magnitude difference as a function of heliocentric distance. Orange filter images with clear filter images taken both before and after were included. A cubic spline was fit to the clear filter images and the interpolated magnitude at the time of the orange filter image was subtracted from the orange filter magnitudes. Error bars were calculated by adding the orange errors and weighted clear errors in quadrature. All C3 orange filter images were half-resolution 512 × 512 images, while all C3 clear and C2 orange filter images were full resolution. Although C3 orange filter images were typically taken as part of a polarizer sequence (no polarizer, 0°, +60°, and −60°), we include only the images with no polarizer.

While there is substantial scatter in Figure 6, the trend is for comets to remain constant or brighten slightly in the orange relative to the clear until a distance of 15–20 $R_\odot$, then fade in the orange relative to the clear interior to this. The vast majority are brighter in the orange than the clear. The exceptions are all images where the comet was marginally observed leaving C3, and are likely due to C3 clear magnitudes which were artificially inflated by an uneven removal of transient solar activity. A quadratic fit weighted by the error bars suggests the peak in the orange relative to the clear occurs at ∼19 $R_\odot$. Biesecker et al. (2002) found a similar color dependence using only C3 orange and clear images for 11 comets observed from 1996 to 1998.

This orange–clear behavior is consistent with the observation that comets fade faster in C2 orange images than in C3 clear images (Section 4.2). It is exhibited by the few comets observed extensively in both orange and clear filters. Figure 7 shows two examples. In the left panel (C/2001 U7 = *SOHO*-365), the orange–clear difference is largest when the comet is first visible in C2 (at ∼10.5 $R_\odot$) and decreases as the heliocentric distance decreases. In the right panel (C/2001 R2 = *SOHO*-347), the orange–clear difference peaks between 15 and 20 $R_\odot$ (note that the comet saturated the detector from 10 $R_\odot$ to 15 $R_\odot$, making these magnitudes unreliable) and is slightly smaller at distances larger than 20 $R_\odot$ and smaller than 10 $R_\odot$.

4.4. Size Distribution

We converted the observed magnitudes to an estimate of the nucleus size by assuming that the brightness is due entirely to the surface area of dust grains in the coma which are reflecting sunlight. For simplicity we assume the coma is optically thin and made of spherical dust grains 1 μm in diameter having albedo 0.04. We then determine the effective radius a sphere of these particles would have been if it disintegrated completely to produce the observed brightness of the comet. Assuming the nucleus has totally disrupted to produce the dust in the coma, we find minimum sizes ranging from 2 m to 50 m in radius.

In this manner, we estimated the size distribution of the Kreutz comets seen by *SOHO*. Ideally, we wish to calculate the size at the peak in brightness. However, because the peak is calculated for less than 10% of our sample, the size distribution calculated from comets observed to peak is inconclusive (Figure 8, left panel).[13] Therefore, we approximate the size distribution by

[13] Here we included the six comets which saturated the detector. While their sizes may be slightly underestimated, their exclusion implies a misleadingly small upper end of the size distribution.

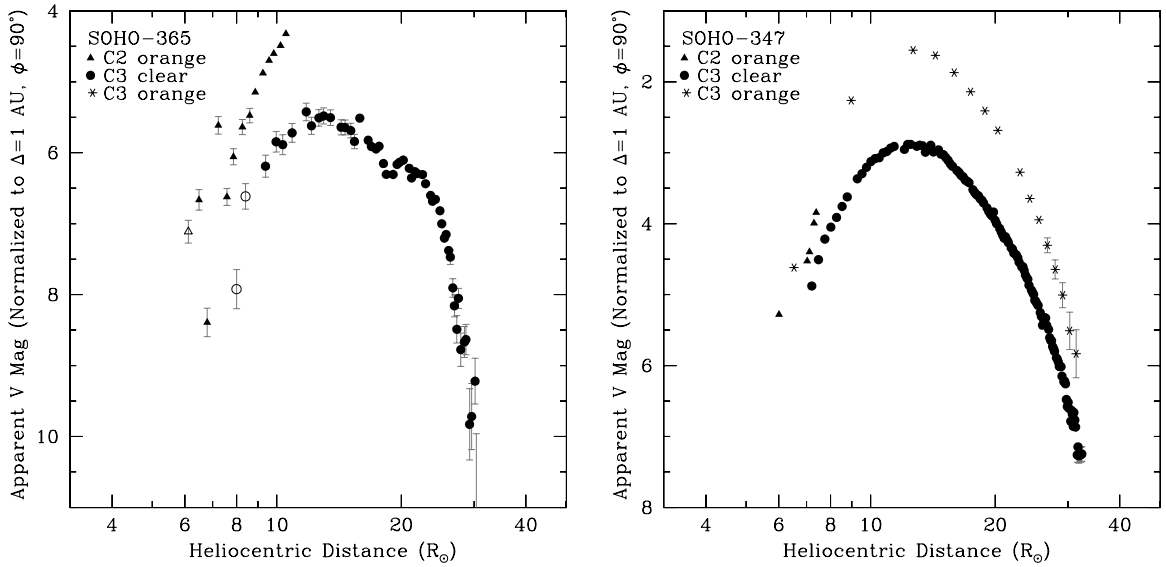

Figure 7. Representative light curves of Kreutz comets with overlapping orange and clear images. The left panel is C/2001 U7 (*SOHO*-365) and the right panel is C/2001 R2 (*SOHO*-347). The symbols are as in Figure 2. Note that C/2001 R2 saturated the C3 detector at its peak, and that the magnitude scales on the two panels are shifted.

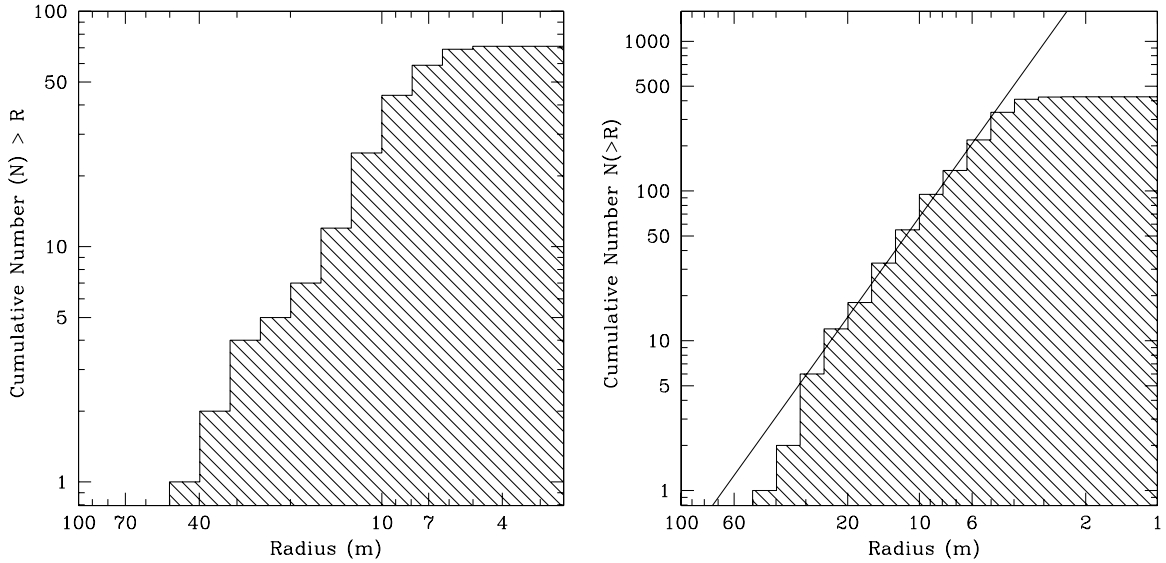

Figure 8. Cumulative size distribution of the comets with a discernible light curve peak in the C3 clear filter (left panel) and the cumulative size distribution based on the brightest point of all comets observed in the C3 clear filter between 10 $R_\odot$ and 15 $R_\odot$ (right panel). Both plots include the six comets which saturated the detector. These represent six of the seven points with sizes greater than 20 m. The line in the right panel is a logarithmic fit from 5 m to 35 m in radius having a slope (log(number) vs. log(radius)) of −2.2.

using all comets which were observed between 10 $R_\odot$ and 15 $R_\odot$ in the C3 clear filter (Figure 8, right panel). While this does not necessarily include the peak brightness for all comets, most are observed very close to their peak, so the distribution should be close to, but somewhat steeper than, the true distribution. We do not include C3 orange filter observations because very few comets were observed in this filter and their inclusion would skew the results toward too many large comets. We do not include C2 observations because most are only observed inside 12 $R_\odot$, and many are too far past their peak brightness, skewing the results toward too many small comets. We fit a line to the data in log(number) versus log(radius) space, with the slope being the power-law exponent. This results in a cumulative size distribution $N(>R) \propto R^{-2.2}$ from 5 m to 35 m in radius. The turnover for sizes smaller than ∼5 m is likely artificial due to incompleteness and the seasonal dependence of the limiting magnitude (discussed in the following section). The lack of comets larger than 30 m may be due to the underestimate of their sizes because these comets saturated the detectors, real and indicative of a turnover in the distribution, or it may simply be small number statistics.

4.5. The Effect of Normalizing the Photometry

As discussed in Section 3.3, we normalized fluxes to unit *SOHO*-centric distance and applied a correction for the phase angle. Since these corrections have a seasonal effect on the light curves, they alter individual light curves differently. The largest effect is generally to the intrinsic magnitude, as comets observed at very large phase angles (greater than 150°) can appear two or more magnitudes brighter than comets observed at intermediate phase angles (30°–100°). This affects the apparent

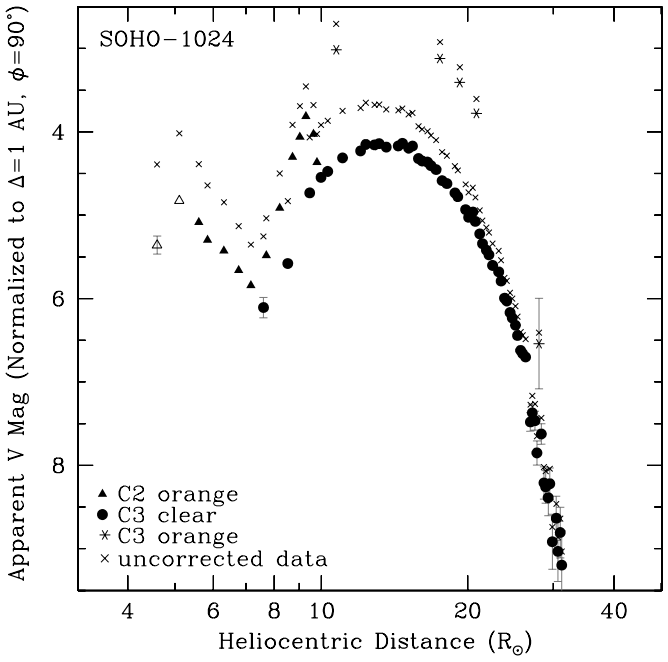

Figure 9. Light curve of C/2005 S1 (*SOHO*-1024) with and without photometric correction. The uncorrected data are plotted as crosses. The corrected data are plotted as in Figure 2.

size distribution of the family. The changing phase angle from image to image can also affect the shape of the light curve, altering the slope of brightening and fading and the distance of the peak of the light curve.

The photometric normalization affects the shape of the light curve of some individual comets strongly. Figure 9 shows the uncorrected (crosses) and corrected (all other points) light curves of C/2005 S1 (*SOHO*-1024). When first visible in C3, its phase angle was 98° resulting in a minimal change in magnitude. The phase angle steadily increased, reaching 128° when last visible in C3 and 143° when last visible in C2, resulting in increasingly larger corrections to the magnitude. After correcting for phase, it appeared to brighten less steeply, fade more steeply, and reach a peak in brightness at a larger heliocentric distance.

While the effect of photometric normalization on individual light curves can be significant, the overall effect on light curve shapes is mitigated by the fact that there are roughly equal numbers of comets made to appear brighter or fainter. The median light curve parameters (Table 3) do not change significantly as a result of the normalization. Furthermore, the distribution of distance of peak brightness is relatively unchanged by photometric normalization, although the median distance is slightly larger and the range of peak distances becomes slightly more spread out.

Since differing δ_{90} values were used for calibrating the clear ($\delta_{90} = 0.52$) and orange ($\delta_{90} = 0.16$) filter images, the orange–clear magnitude differences are affected even though they are interpolated from clear filter images at the same time (and thus phase angle) as the corresponding orange filter images. The change is equal to the difference between the $\delta_{90} = 0.52$ and $\delta_{90} = 0.16$ lines in Figure 1. For phase angles (θ) smaller than $\sim 100°$, the change is less than ± 0.1 mag. For $\theta > 100°$, the correction is larger in the clear filter than the orange, hence the orange–clear color difference increases, with an increase of ~ 0.5 mag for $\theta > 130°$. About half of the orange–clear points have a phase-induced magnitude change less than ± 0.1 mag, however, due to the asymmetry of the phase correction, the average correction to the orange–clear magnitude was -0.16 mag. As a result of the phase correction, the orange–clear magnitude difference is larger than in the uncorrected data, meaning a larger fraction of the light is due to sodium than would be inferred from the uncorrected data.

The limiting magnitude of both C2 and C3 is approximately 8. In practice, C2 is more sensitive to comets in the range 7–8 mag than C3 because of its smaller pixel scale and better signal to noise, making detections easier. We believe the data set is relatively complete for comets brighter than apparent magnitude 7 in C3 and apparent magnitude 8 in C2. The correction for Δ and phase (Figure 10) reveals that the distribution of intrinsic magnitudes is not as clear cut. A significant number of comets intrinsically too faint to be seen by *SOHO* are made bright enough to be visible due to phase effects (the excess of comets at magnitudes fainter than 8 in the histograms, with hatching at +45°). Roughly equal numbers of comets experience phase related brightening and fading. However, due to the asymmetric effect of scattering, comets may appear $\sim$2 mag brighter but only $\sim$0.1 mag fainter. Since the most a comet would appear fainter due to phase is $\sim$0.1 mag, the limiting magnitudes to which the distribution is complete are essentially unchanged, $\sim$8 in C2 and $\sim$7 in C3. The turnover in the distribution for magnitudes fainter than this is a combination of the sensitivity of the detectors and the effects of the phase angle. The substantial numbers of magnitude 9–10 comets observed, despite the limited annual times when these comets are visible, suggests that there are larger numbers of comets at fainter magnitudes.

Despite significant changes to the magnitude distribution due to the phase correction, the slope of the size distribution is unchanged. For all comets seen in the C3 clear filter from 10 $R_\odot$ to 15 $R_\odot$, both the uncorrected and corrected data sets yield a slope of -2.22 for nuclei of radius 5–35 m. For comets brighter than the completeness limit for C3 (magnitude 7, which corresponds to a 4.9 m radius), the phase angle affects the same proportion of comets of all sizes.

5. DISCUSSION

5.1. Orange–Clear Magnitude Difference

The comets appear brighter in the orange filter than the clear filter by about 1 mag. This difference is due to emission in the orange bandpass which is much brighter in proportion to the reflected solar continuum in the narrower orange bandpass than it is to the reflected solar continuum across the wider clear bandpass. The emission seen in Kreutz comets consists of the bands typically observed in comets at larger heliocentric distances (e.g., CN, C_2, etc.), ions not seen at larger distances, and elements seen in the spectra of sungrazers ([O I], Na I, K I, Ca II, Cr I, Mn I, Fe I, Ni I, Cu I, and CN were reported in Ikeya-Seki by Preston 1967 and Slaughter 1969). Of the emission lines seen in Ikeya-Seki, only [O I] (6300 Å) and Na I (5890 Å and 5896 Å) fall within the orange filter bandpass (5400–6400 Å). Since sodium is much brighter than the forbidden oxygen line, it is the most likely source for the excess brightness in the orange filter relative to the clear filter.

To test this, we estimated the increase in the sodium line relative to the solar continuum required to cause the orange filter to increase by $\sim$1 mag relative to the clear filter. We calculated the flux due to reflected solar continuum in each detector/filter combination (C3 clear, C3 orange, C2 orange) by multiplying

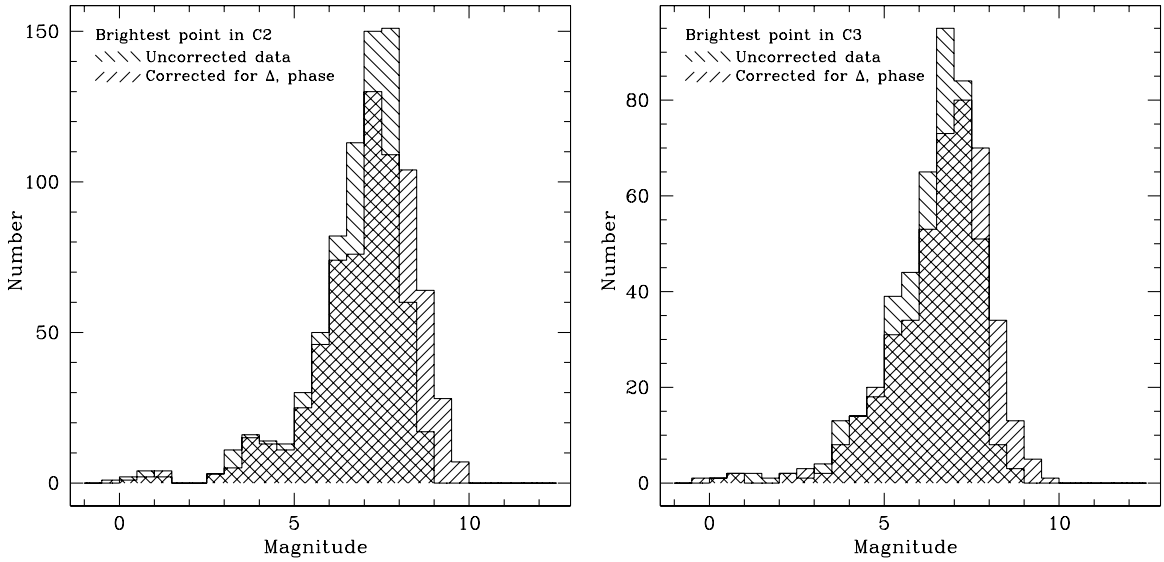

Figure 10. Histogram of brightest magnitude for comets observed in C2 (left panel) and C3 (right panel). The uncorrected size distribution has hatching going at −45° and the data corrected for phase angle and *SOHO*-centric distance has hatching at +45°. Note that the scales are different because more comets are seen in C2 than in C3.

the solar flux at each wavelength[14] by the transmission of the filter at that wavelength[15] and the quantum efficiency of the detector at that wavelength.[16] We then simulated the flux of sodium emission by adding a rectangle of width 10 Å centered at 5895 Å (to encompass both sodium D-lines) and of a variable height. The apparent magnitude was ∼1 mag brighter in the orange filters relative to the clear filter for a height of sodium emission ∼600 times stronger than the solar continuum at 5895 Å. The integrated flux due to the sodium emission was ∼1.9 times more than the integrated flux due to the solar continuum in the clear filter and ∼6.4 times more in the orange filter.

To convert this to an estimated mass of sodium, we estimated that the contribution from the sodium emission was 1.9/(1 + 1.9) of the total flux received by *SOHO* from the comet in the C3 clear filter. Next, we divided the total flux of the comet by the *g*-factor for sodium,[17] and converted this to a mass of sodium. For a fifth magnitude comet, this yields a mass of ∼1000 kg. The photoionization lifetime of sodium at 12 $R_\odot$ is ∼9 minutes, after which the sodium ion rapidly leaves the photometric aperture. Therefore, a production rate of ∼2 kg s^{-1} is required to sustain the brightness. In this manner, we integrated the sodium production for the light curve of C/2005 S1, which was observed in C3 from 31.2 $R_\odot$ to 7.6 $R_\odot$ over 33 hr and reached a peak magnitude of ∼4.5 at 14 $R_\odot$. During this time it produced 1.7 × 10^8 g of sodium. This is a large fraction of the estimated mass of C/2005 S1 (4 × 10^9 g using the estimated size and a density of 0.35 g cm^{-3}). However, if the nucleus is a factor of 2 larger, the sodium would represent less than 1% of the mass. This begins to be plausible, but it may imply that our size estimates are too small.

It is likely that emission from other atoms or molecules besides sodium contributes to the overall brightness. However, the ∼1 mag orange–clear difference indicates that emission in the orange filter bandpass is the dominant emission in the visible range. It is also possible that as yet unidentified refractory silicates are responsible for emission in the orange filter bandpass. While we cannot rule out this possibility, the observations of strong sodium emission at small heliocentric distances in Ikeya-Seki (Curtis & The Sacramento Peak Observatory Staff 1966; Evans & McKim Malville 1967; Preston 1967; Spinrad & Miner 1968; Slaughter 1969) and C/2006 P1 McNaught (Snodgrass et al. 2007; A. Voulgaris 2007, private communication) confirm that sodium emission should be extremely bright at the distances observed by *SOHO*.

An alternative explanation of the orange–clear magnitude difference is improper photometric normalization. The photometric zero points were calculated using thousands of images of dozens of F, G, and K stars repeated annually over the life of the mission (Llebaria et al. 2006; Thernisien et al. 2006; A. Thernisien 2003, private communication). We consider the zero points to be reliable and conclude that the orange–clear magnitude difference is a real effect diagnostic of differences in the flux from that of the solar continuum.

5.2. Nucleus Sizes

Coronagraphically observed Kreutz comets have consistently been estimated to be a few meters to tens of meters in size. MacQueen & St. Cyr (1991) estimated the brightest *SMM* comets to be ∼16 m in radius prior to the onset of sublimation. Lyα fluxes recorded by UVCS have yielded estimates of the diameters of three comets at distances from 3 $R_\odot$ to 7 $R_\odot$: 6.7 m for C/1996 Y1 at 6.8 $R_\odot$ (Raymond et al. 1998), 5.0–6.7 m for C/2000 C6 at 6.36–5.71 $R_\odot$ (Uzzo et al. 2001), and 7.8 m (with an unresolved 5.4 m companion) for C/2001 C2 at 4.98 $R_\odot$ (Bemporad et al. 2005). Sekanina (2003) estimated initial diameters ranging from 17 m to 200 m by modeling 27 light curves with varying effective latent energies of erosion (analogous to sublimation heat). Iseli et al. (2002) used the fact that no Kreutz comets have been seen by *SOHO* after perihelion

[14] We used the 1985 Wehrli Standard Extraterrestrial Solar Irradiance Spectrum from http://rredc.nrel.gov/solar/spectra/am0/wehrli1985.new.html.
[15] http://lasco-www.nrl.navy.mil/index.php?p=content/filter/filter.
[16] http://lasco-www.nrl.navy.mil/content/tech/QE.
[17] The *g*-factor is the emission rate per molecule. We estimated it to be 5.5 × 10^{-11} erg s^{-1} $atom^{-1}$ at 1 AU from Figure 2 in Watanabe et al. (2003) and scaled it by r^{-2} to 12 $R_\odot$. Note that the radial velocity of a typical Kreutz comet at this distance is ∼230 km s^{-1}, which is well beyond the dip in the *g*-factor due to the Swings effect.

to derive an upper limit for the radius of 63 m if it was composed entirely of water ice and destroyed by sublimation alone. Our estimate of the size distribution, ranging from 2 m to 50 m in radius, is consistent with these values. However, the nuclear sizes are likely good to within a factor of 2 due to a number of uncertainties, and the actual size range may be 1–100 m in radius. Below, we consider the validity of the assumptions used to calculate this size distribution.

First, we assumed that the brightness is due entirely to the reflection of sunlight off dust grains in the coma. In actuality, the brightness is a combination of scattering off the coma, scattering off the nucleus, and emission. A bare nucleus 50 m in radius should have an apparent magnitude of ∼18 at 12 $R_\odot$. Since the faintest comets observed are approximately magnitude 9, we can safely ignore the nucleus contribution. We have shown above that sodium emission likely represents a substantial fraction of the brightness. Since our size estimate has assumed that all brightness comes from dust, this makes our size estimates too large.

A second assumption is that the comet has disintegrated completely into dust at the distance of peak brightness (10.5–14 $R_\odot$). This is very likely not the case, as UVCS observations indicate the presence of a nucleus in all three comets observed by it at distances inside 7 $R_\odot$, although the nuclei are believed to have fragmented or sublimated completely by ∼3 $R_\odot$ (Raymond et al. 1998; Uzzo et al. 2001; Bemporad et al. 2005). If the nucleus has not been completely destroyed at the distance of peak brightness, then we have underestimated the total size of the nucleus plus coma.

Because so few comets are observed well enough to determine a peak in the light curve, we have calculated the size distribution using all comets seen between 10 $R_\odot$ and 15 $R_\odot$. Since these are all observed near their peak in brightness, the size distribution should be close to the true distribution. However, since most of these light curves are incomplete, any additional observations would only make the inferred sizes larger since observations fainter than the brightest observed magnitude would not be used. Thus, the sizes of the incompletely observed comets are somewhat larger than estimated here.

If we assume the comet is made entirely of water ice, and scale the water production rate from 10^{18} molecules s^{-1} cm^{-2} at 1 AU by a factor of r^{-2}, a comet which is ∼50 m in radius when it enters the *SOHO* field of view will decrease in radius by 16 cm hr^{-1} at 30 $R_\odot$, 36 cm hr^{-1} at 20 $R_\odot$, and 143 cm hr^{-1} at 10 $R_\odot$ (assuming a density of 0.35 g cm^{-3}). If we further assume the comet has a rotation period of 1 day, a thermal inertia of 50 W K^{-1} m^{-2} $s^{0.5}$ (the upper limit for the thermal inertia of 9P/Tempel 1; Groussin et al. 2007), and heat capacity C_p = 2.05 J g^{-1} K^{-1}, its skin depth would be ∼1 cm. Even if the heat capacity is lower and the rotation period longer, the skin depth would not be more than 3–5 cm for reasonable values. Thus, the rate of erosion in the *SOHO* field of view is much larger than the skin depth. As a result, no volatile depleted mantle can form and the erosion exposes fresh ices which were buried below the surface until very recently.

As an analog, we use the ejecta released by the Deep Impact experiment which excavated nearly pristine ice below the surface of 9P/Tempel 1, resulting in a size distribution that was smaller than the ambient pre-impact coma and rich in water ice (e.g., Sunshine et al. 2007; Knight et al. 2007; Schulz et al. 2006; Fernández et al. 2007). Lisse et al. (2006) found that the Deep Impact ejecta were dominated by 0.1–10 μm particles, with a peak in the size distribution at 1 μm. Our size estimate assumed that the coma was optically thin and consisted of uniform spheres of diameter 1 μm. Modeling the coma with a distribution of particles of diameter 0.1–10 μm might improve the size estimate, but the uncertainties inherent in this estimate make an overly specific particle size distribution superfluous. Equivalent nuclear radii constructed entirely from spheres of diameter 0.1 μm or 10 μm differ from the 1 μm equivalent nuclear radius by a factor ∼2–3 (smaller particles have a larger surface area to volume and result in a smaller equivalent nucleus and vice versa).

We used an albedo of 0.04, as is commonly assumed for comets. However, all previous albedo measurements have been made at much larger heliocentric distances (e.g., A'Hearn et al. 2005). The low albedo of comets is believed to be due to organics, but at the heliocentric distances observed by *SOHO* the organics likely sublimate very soon after being exposed to sunlight. Thus, the albedo of the dust may be higher than assumed, and the comet may be smaller than that inferred from our estimates.

5.3. Size Distribution

The size distribution exponent $\alpha = 2.2$ is similar to the slope of the Jupiter family comets which is 1.73–1.91 (Meech et al. 2004; Lamy et al. 2004; Weissman & Lowry 2003) or 2.65–2.70 (Fernández et al. 1999; Tancredi et al. 2006). After accounting for the effects of fragmentation and sublimation, Lowry et al. (2008) estimate that the primordial slope was 1.83–2.01. The two populations were produced by different mechanisms (splitting for the Kreutz comets versus collisions for the Jupiter family comets), but it is nonetheless interesting that the slopes are similar. If the comets were allowed to continue in their orbits instead of disintegrating on the subsequent perihelion passage, they would likely continue to fragment, steepening the slope of the size distribution. If it is assumed that the cometesimals which formed the original Kreutz progenitor have maintained their integrity (their internal strength is stronger than their connection to neighboring cometesimals), then continued fragmentation should cause the size distribution to reflect the true size distribution of the cometesimals where the Kreutz progenitor formed.

The Weidenschilling (2004) two-dimensional model for the formation of comets predicts they are composed of components ranging in size up to ∼100 m. Thus, the size distribution seen in the Kreutz today may be close to the primordial distribution, and the discontinuity in the cumulative size distribution between the ground-observed and *SOHO*-observed comets (discussed in the following section) may be reflective of two distinct populations: large bodies composed of 1–100 m components and the components themselves. The consistency of our size estimates with those estimated for the fragments of disrupted comets D/1999 S4 LINEAR (25–60 m) and 73P/Schwassmann-Wachmann 3-C (of order 10 m; Weaver et al. 2001, 2006) suggests that we are seeing the constituent cometesimals.

5.4. Distribution Around the Orbit

To estimate the total mass of the Kreutz system, we need to correct for the comets which were unobserved due to data gaps. From 1996 to 2005, the collective duty cycle for C3 with the clear filter was 0.868. We do not need to correct for the seasonal effects because our size distribution was calculated using only the comets which were large enough to have been observed

regardless of the geometry. Over 10 years, we observed 219 comets bigger than 5 m. Assuming a continuous distribution of comets throughout the orbit, this represents 0.868 of the total observable. For an 800 year orbit, this yields ∼20,000 comets larger than 5 m in radius in the orbit. The cumulative size distribution is

$$N(>R) \approx 869 \times R^{-2.2}, \quad (2)$$

where $N(>R)$ is the number of comets year^{-1} larger than radius R (in meters) which reach perihelion. For a density of 0.35 g cm^{-3}, this converts to a cumulative mass distribution of

$$N(>m) \approx 2.1 \times 10^{7} m^{-0.73}, \quad (3)$$

where $N(>m)$ is the number of comets year^{-1} larger than mass m (in grams) which reach perihelion.

Extending Equation (2) to radii larger than 3.6 m (which correspond to comets ∼8th magnitude or about the nominal limiting magnitude of C3), we should have observed 267 comets 3.6–5.0 m in radius from 1996 to 2005, but we only saw 162. Even after correcting for the duty cycle, ∼30% of the expected comets in this range were unobserved. This is largely due to the viewing geometry, but is also due to the limited amount of time over which comets attain their peak brightness. A comet is required to be in at least five images to be confirmed by the *SOHO* team.[18] An average of 2–3 C3 clear images are taken per hour. Thus, the comet must be above the minimum threshold for ∼2 hr to be discoverable. Near the light curve peak, the comet will travel ∼2 $R_\odot$ in two hours. So, for comets near the limiting magnitude, if the brightness peaks steeply the comet will not be detected, but if it has a broad peak it may be detected. Many of the faintest detections appear this way—they have no discernible slope, just 5 or so points barely above the limiting magnitude.

There are also fewer comets larger than 30 m than expected. This may be because these comets saturate the detector, causing their sizes to be underestimated. However, we would then expect a surplus of comets slightly smaller than 30 m. Since no excess is seen, the deficit of large comets appears real. From the size distribution, we would expect 4.6 such comets in 10 years, while only two were seen. We tested the likelihood that the comets larger than 30 m are from the same distribution as those smaller than 30 m by assuming that an average of 0.00126 comets bigger than 30 m arrives on a give day (4.6 comets in 10 years). We then generated a random number for each day for 10 years to determine whether or not a comet arrived on that day, and repeated the simulation 10,000 times. 16.2% of the time the simulation resulted in two or fewer comets 30 m or larger. Thus, until the baseline of observations is increased, we cannot conclude that there are significantly fewer comets larger than 30 m, and hence a break in the power law around 30 m.

Assuming the distribution of comets seen by *SOHO* is constant throughout an 800 year orbital period and setting $N(>R) = 1$, we would expect the largest comet to have a radius of ∼500 m. For comparison, we used the light curve parameters given by Sekanina (2002a) to estimate the sizes and masses of the ground-observed Kreutz comets (Table 1).[19] The size distribution cannot explain the six comets larger than 1 km, as we would expect ∼0.1 such comets in 800 years. We simulated this as above, assuming the size distribution holds at all sizes and the baseline over which comets bigger than 1 km have reliably been detected is 200 years. None of our 1000 simulations had more than one comet arrive during 200 years.[20] Even if our rough estimates of the nuclear sizes are an order of magnitude too large, we are still left with 3–4 comets larger than the expected maximum size. Thus, we conclude that there is a break in the size distribution which occurs by 500–1000 m in radius and possibly as small as 30 m. However, we note that the distribution seen by *SOHO* may not be representative of the distribution at other times.

Integrating over the size range 5–500 m we find the total mass for the *SOHO*-discovered comets to be ∼4 × 10^{14} g for a bulk density of 0.35 g cm^{-3}, equivalent to a sphere of radius ∼650 m. The total mass is dependent on the upper cutoff of the size distribution, so if the maximum size is smaller than 500 m, the total mass of the system will be lower. Therefore, the inferred total mass of the population of coronagraphically observed fragments is much smaller than the mass of any of the bright ground-observed comets (∼10^{15}–10^{19} g). This is further evidence that the *SOHO*-observed Kreutz comets are "debris" in the system.

5.5. Rate of Brightening

Of the ground-observed Kreutz comets, only Ikeya-Seki was well observed prior to perihelion, while five were observed after perihelion (Table 1). The fading rate for the ground-observed Kreutz comets was between $r^{-3.2}$ and $r^{-4.5}$, which is similar to the brightening rate we derived from 16 $R_\odot$ to 24 $R_\odot$ for the comets observed by *SOHO* ($\propto r^{-3.8\pm0.7}$). Despite being observed at much larger heliocentric distances, the brightness behavior of the largest comets (all of which survived perihelion) is similar to that of the smallest. From this we conclude that the brightening seen in the *SOHO* field of view from 16 $R_\odot$ to 24 $R_\odot$ is typical for all Kreutz comets rather than due to processes which are unique to the smallest comets, such as catastrophic disruption and subsequent disintegration.

The *SOHO*-observed Kreutz comets brighten $\propto r^{-7.3\pm2.0}$ beyond ∼24 $R_\odot$. Ikeya-Seki brightened at a rate near r^{-4} from 1.02 AU to 0.03 AU (Sekanina 2002a and references therein). Unfortunately, it was not observed from 50 $R_\odot$ to 20 $R_\odot$ prior to perihelion. After perihelion there were nine observations from 9 $R_\odot$ to 50 $R_\odot$, including three between 20 $R_\odot$ and 40 $R_\odot$. The light curve fluctuates about the r^{-4} line, but there is no obvious section which fades significantly steeper than this. If Ikeya-Seki experienced a significant period of brightening near $\sim r^{-7}$, it only occurred prior to perihelion and only from 50 $R_\odot$ to 20 $R_\odot$. Thus, we cannot determine when the $\propto r^{-7.3}$ brightening begins, but conclude it is unlikely to extend beyond 50 $R_\odot$.

Sekanina (2000b) examined the tail morphology of nine Kreutz comets observed from 1996 to 1998, finding that the production of dust peaked at 20–30 $R_\odot$ and had $\beta \leqslant 0.6$ (β is the ratio of the force due to solar radiation pressure and the force due to the Sun's gravity). The distances of peak production correspond to the approximate locations of the changes in slope from $\propto r^{-7.3}$ to $\propto r^{-3.8}$. We compared the light curves of the nine comets in the Sekanina (2000b) study with their inferred

[18] Occasionally, comets with fewer than five images have been confirmed. All of these clearly show cometary activity and were only in fewer than five images because the rate of C2 images was low.

[19] The magnitudes for the 19th century comets are generally for the nuclear condensation, while for the 20th century comets, integrated magnitudes are given. The *SOHO* photometry uses a fixed aperture which more closely resembles the nuclear condensation. The integrated magnitudes imply brighter comets than the nuclear condensation. For this order of magnitude calculation, it is sufficient to assume they are equivalent.

[20] If the near-Sun comets observed since the 16th century and considered as possible Kreutz comets by Sekanina & Chodas (2007) are included, 23 additional massive comets are in the group and the size distribution fails miserably for large comets.

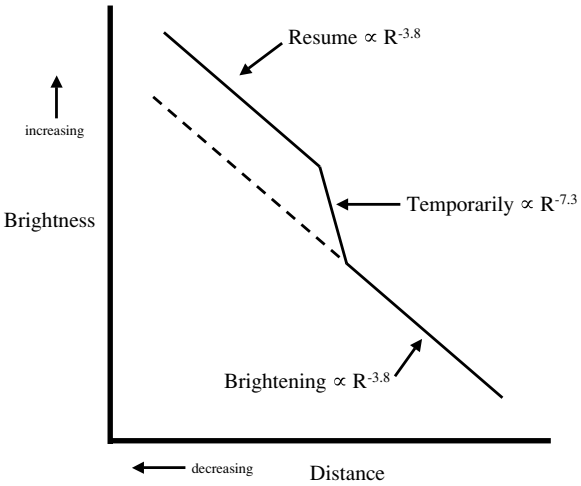

Figure 11. Illustration of the Kreutz brightening rate.

distance of peak dust production. While eight of the nine comets in the sample exhibited a change of slope between 20 $R_\odot$ and 30 $R_\odot$, the distances were uncorrelated with the inferred peak production distance.

The steep rate of brightening is likely due to the onset of activity of a previously inactive species (presumably a refractory organic) which results in an explosive outburst. In this scenario, the increasing insolation causes a buildup of pressure below the surface. At some point, the pressure exceeds the strength of the regolith and an outburst blows off much of the outer layer. The destruction of the regolith would deposit a large amount of small silicate dust grains into the coma, and the surface area of the coma would continue to increase for some time while the ejected dust fragmented. As fragmentation slows, the comet returns to its $\propto r^{-3.8}$ brightening, offset brighter if the active surface area has increased as a result of the outburst. Alternatively, the onset of activity may trigger the entire nucleus to become active rather than just a few regions. The resulting light curve is illustrated in Figure 11.

To test the rate of brightening beyond the *SOHO* field of view, we surveyed regions of the sky statistically likely to contain Kreutz comets approximately three–six months prior to perihelion using the MOSAIC camera on the KPNO 4 m telescope. We aligned three consecutive images and blinked them to look for moving objects. Later, as comets were discovered by *SOHO* which should have been in the field of view, we searched the images again to look for comets near the expected positions. While as many as 12 comets may have been in the field of view, none were found. This suggests that they either brightened at a rate steeper than $\propto r^{-3.5}$ or that the orbital element uncertainties are larger than we had estimated. Additional fields at a different epoch provided by Scott Sheppard and Chad Trujillo using the Magellan 6.5 m telescope at Las Campanas also did not reveal any comets.

5.6. Qualitative Explanation of the Light Curve

Previous interpretations of the light curves of the Kreutz group have focused on the apparent bimodality of the peak in brightness noted by Biesecker et al. (2002). Sekanina (2003) has explained the differences as corresponding to comets having differing latent energies of erosion, and in some cases additional fragments too small or too recently separated to be individually resolved. Kimura et al. (2002) attribute the two peaks as corresponding to fluffy aggregates of crystalline olivine (the peak at 11.2 $R_\odot$) and fluffy aggregates of amorphous olivine (the peak at 12.3 $R_\odot$). They further argue that the observed light curves are a superposition of two light curves: one due to olivine which peaks from 10 $R_\odot$ to 13 $R_\odot$ and one due to pyroxene which peaks inside 7 $R_\odot$, with the relative heights of the peaks at ∼12 $R_\odot$ and inside of 7 $R_\odot$ indicative of the abundance ratio of olivine to pyroxene.

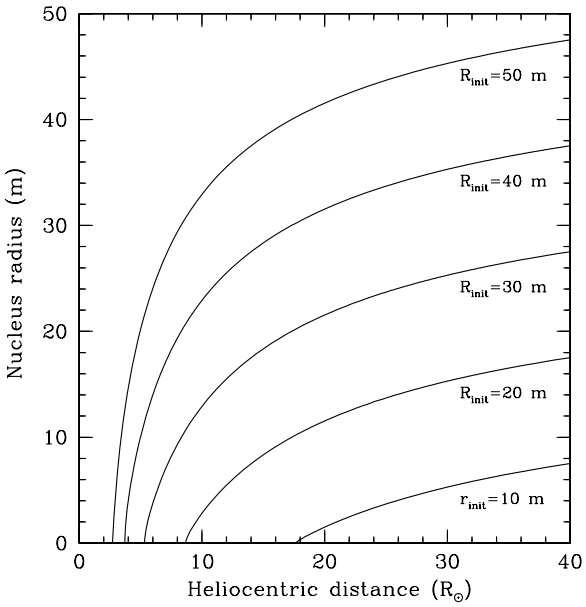

Figure 12. Decrease in size of a Kreutz nucleus due to water production. The initial sizes listed for each curve were the sizes four days prior to perihelion at a distance of ∼58 $R_\odot$. The comet follows the orbit of C/1963 R1 Pereyra which is very close to the "subgroup I" orbit (Marsden 1967) of most *SOHO*-observed comets. The nucleus is assumed to be composed entirely of water, and the water production rate is scaled from 10^{18} molecules s^{-1} cm^{-2} at 1 AU by a factor r^{-2}.

Our analysis shows that the distance of peak brightness is not bimodal, but is more nearly a Gaussian centered near 12 $R_\odot$ and ranging from 10 $R_\odot$ to 14 $R_\odot$. Without the need to explain two distinct light curves, this can now be viewed as reflecting a collection of comets with similar compositions that behave slightly differently due to their unique fragmentation history, topography, rotation, etc. Rather than being confined to two narrow ranges, the peak distances actually vary over a fairly large region, representing a change of ∼30% in heliocentric distance between the largest and smallest peak distances.

We demonstrated that rather than the two "universal curves" which were discriminated by distance of the peak, the light curves have a continuum of shapes. These shapes can be explained by compositions with varying ratios of amorphous and crystalline olivines. Kimura et al. (2002) showed that amorphous olivines sublimate more slowly and at larger distances than crystalline olivines. Thus, the comets we classified as belonging to group A have higher ratios of amorphous olivines to crystalline olivines than the comets in group B, which in turn have higher ratios than group C.

There does not appear to be a correlation between size of the nucleus and the distance of peak brightness. We would expect a size dependence since bigger comets take longer to erode and therefore survive to a smaller heliocentric distance. However, as shown in Figure 12, if the erosion is dominated by water production, nuclei of nearly all sizes will survive until heliocentric distances smaller than the light curve peak at 10.5–14 $R_\odot$. The smallest nuclei will erode prior to the peak distances,

but these are below the threshold for detection and therefore do not appear in our database. Since the distance of the light curve turnover does not correlate with the size estimate, the destruction of the nucleus by erosion is not the primary cause of the light curve turnover.

As explored by previous authors (e.g., Biesecker et al. 2002; Kimura et al. 2002), the light curve shape is an amalgamation of numerous processes which depend on the heliocentric distance. These include but are not limited to the production of water and other volatiles from the nucleus, emission of sodium and other heavy elements, the sublimation of olivine, pyroxene, and other silicates from the coma and the nucleus, the photoionization lifetimes of particles in the coma, fragmentation, and tidal forces on the nucleus. Undoubtedly the unique evolutionary history of each comet contributes to its distinct shape, but we can explain the general shape as follows.

At large heliocentric distances, the comets behave like dynamically young comets, rich in ices and with a small dust size distribution due to splitting events since the previous perihelion passage which expose new surfaces, e.g., Sekanina (2000a, 2002b). Beyond 50 $R_\odot$, they likely brighten at a rate near $\propto r^{-4}$ as Ikeya-Seki did (Sekanina 2002a). Although it is unclear exactly where, at some point prior to entering the *SOHO* field of view, most begin to brighten steeply, near $\propto r^{-7.3}$. This continues until ~24 $R_\odot$ when the rate rapidly transitions to $\propto r^{-3.8}$.

Around 16 $R_\odot$ the light curve begins to turn over, reaching a peak between 10 $R_\odot$ and 14 $R_\odot$. Kimura et al. (2002) showed that sublimation of fluffy aggregates of amorphous and crystalline olivine occurs at 10–13 $R_\odot$. This will rapidly deplete the reflecting area of the coma. While the production rate (per cm^2) is increasing $\propto r^{-2}$, at some point the surface area of the nucleus becomes too small and the total production drops. The combination of a declining production rate and an increasing sublimation rate causes the light curve to turn over and fade rapidly.

Inside of ~7 $R_\odot$, the comet will erode very rapidly. UVCS observations of three comets suggest that the nuclei disappear entirely by ~3 $R_\odot$ (Raymond et al. 1998; Uzzo et al. 2001; Bemporad et al. 2005). Kimura et al. (2002) predict that the sublimation of crystalline and amorphous pyroxenes (which sublimate around 5 $R_\odot$) would cause a second peak at 4–6 $R_\odot$. The light curves in this region are sparse, but are in general agreement with this as the light curves tend to level off or brighten again inside ~7 $R_\odot$. An alternative explanation for this phenomenon is that fragments too small to be individually resolved, and which have substantially higher erosion energies, reach a peak in brightness in this region (Sekanina 2003). Since the range of peak distances indicates that the comets are relatively homogeneous, we find it unlikely that they would fragment into pieces with such disparate energies of erosion. Therefore, we favor the final disruption of the nucleus and sublimation of pyroxene as the mechanism to cause this final brightening.

5.7. Light Curve Behavior for the Comets Beyond the Sizes *Seen By* SOHO

The scenario described above should hold true for comets in the size distribution observed by *SOHO*. Comets with initial radii smaller than a few meters would be destroyed by erosion at larger distances than 10–14 $R_\odot$. These comets would never achieve the brightness necessary to be observed by *SOHO*, however if the size distribution holds, they should be numerous. While the nucleus of such a comet would have disrupted, the dust should continue along the orbit subject to the effects of radiation pressure. Thompson (2009) showed that the tail of comet C/2007 L3 consisted of particles emitted between 18 and 24 hr before perihelion (18–22 $R_\odot$) and which persisted until several hr after perihelion. Similarly, the tail of C/1979 Q1 was evident for 100 minutes after perihelion in *Solwind* images (Michels et al. 1982), and we have noted the phenomenon in a number of bright *SOHO* comets. Future coronagraphic missions with greater sensitivity might observe the tails of comets too small for the nucleus to have survived into the *SOHO* field of view as headless comets.

A comet large enough to survive until a subsequent return (radius ~500 m according to Sekanina 2003) should peak in brightness at perihelion and brighten and fade symmetrically, as did Ikeya-Seki. We would expect surges in brightness as olivine and pyroxene begin to sublimate at 10–14 $R_\odot$ and 4–6 $R_\odot$, respectively. A comet large enough to survive perihelion, but which eroded away soon after (radius ~250 m according to Sekanina 2003) would fade more steeply than it brightened. It is possible that C/1887 B1 was such an object, being large enough to survive perihelion, but having no nucleus (or one so small that it was not outgassing appreciably).

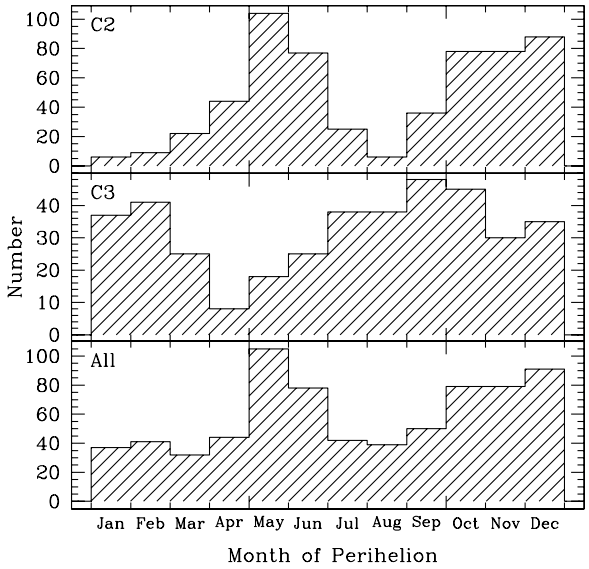

Figure 13. Histogram of the month of perihelion for Kreutz comets observed by *SOHO* from 2004 to 2008. The top panel shows comets observed in C2. The middle panel shows comets observed in C3. The bottom panel shows all comets, regardless of telescope. Note that the total number is less than the sum of C2 and C3 because many comets are seen in both telescopes.

6. POPULATION

6.1. Seasonal Variability

There is a distinct seasonal variation in the observation rates of Kreutz comets (Figure 13). Observations of comets in C2 (these comets may or may not be seen in C3) peak strongly from April to June and again from October to December each year, while C3 observation rates (these comets may or may not be observed in C2) are more constant, but dip from March to June and November to December. The combined discovery rate is relatively flat, with peaks that mirror the peaks in C2. This seasonal variability is due to the combination of two factors: the geometry of the Sun–*SOHO*–Kreutz system and the brightness behavior of Kreutz comets at small heliocentric distances. We discuss these effects below, and summarize them in Table 4.

Table 4
Summary of Seasonal Effects on Detection Rate

Effect	When	C2 Discovery Rate	C3 Discovery Rate
Occulting arm	Jan–May	Small decrease	Large decrease
Telescope roll	Every 3 months	Small increase when rolled in Jan–May	Large increase when rolled in Jan–May
SOHO–Sun line nearly in the plane of Kreutz orbit	Apr–Jun and Oct–Dec	Large increase	Slight decrease
SOHO–Sun line nearly perpendicular to the plane of Kreutz orbit	Jan–Mar and Jul–Sep	Large decrease	Slight increase
Phase angle	Sep–Jan	No change	Increase
Phase angle	Aug–Dec	Increase	No change
SOHO–comet distance <1 AU	Sep–Mar	Slight increase	Slight increase
SOHO–comet distance >1 AU	Apr–Aug	Slight decrease	Slight decrease

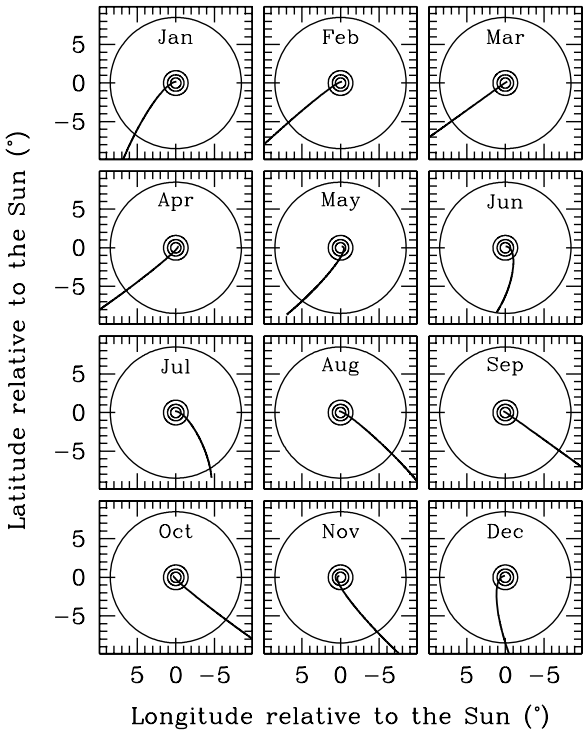

Figure 14. Monthly track across the *SOHO* coronagraphs for typical Kreutz comets. The track is for a comet which reaches perihelion on the 15th day of the month specified in each plot. The heavy line is the last three days of the orbit prior to perihelion. The post-perihelion track is not plotted since no Kreutz comets have been seen by *SOHO* after perihelion. The circles represent the edges of the coronagraphs. Starting from the largest circle they are C3 outer, C2 outer, C3 inner, and C2 inner.

6.1.1. Obstruction by the Occulting Arm

Kreutz comets approach the Sun from the south (the bottom of unrolled *SOHO* images when north is up and east is to the left). Figure 14 shows the monthly track of a typical Kreutz comet through the *SOHO* field of view. The occulting arms on C2 and C3 extend from the bottom left corner to the middle at roughly a 45° angle in unrolled images, and from the top right in rolled images. Thus, comets which arrive from January to early May frequently cross the occulting arm in unrolled images. This reduces the counts recorded, sometimes completely obscuring the comet and preventing detections. This has a minimal effect in C2, but is strong in C3 where the vignetting is more severe, and results in a lower discovery rate during these months.

This effect has been mitigated since mid-2003 by the 180° rolls performed every ∼3 months. When the telescope is rolled, the occulting arm extends from the northwest and does not cross the Kreutz track. This has improved the discovery rate during times when the track is usually obstructed by the occulting arm. This effect can be seen in the C3 discoveries in January to April in Figure 13. During this time, *SOHO* has always been rolled in January and February, has been rolled about half the time in March, and has never been rolled in April.

6.1.2. Elongation of Peak Brightness

A second effect of the geometry is on the elongation at which the Kreutz comets reach peak brightness (Figure 15). The *SOHO*–Sun line is approximately in the plane of the Kreutz orbit from April to June and October to December. During these months, comets approach the Sun from behind (April to June) or in front (October to December), and reach their peak brightness at a smaller solar elongation. At these times, typical Kreutz comets are at a heliocentric distance of 8.5–12 $R_\odot$ when they enter the C2 field of view, making them visible in C2 at or soon after their peak brightness. From January to March and July to September, the *SOHO*–Sun line is roughly perpendicular to the plane of the Kreutz orbit. During these months, typical Kreutz comets are at a heliocentric distance of 6–7 $R_\odot$ when they enter the C2 field of view. Thus, they do not appear in C2 until well after peak brightness, and fewer comets are visible. The heliocentric distance at which comets leave C2 has no effect on discovery rates, as only the very brightest comets are still seen leaving C2.

This plane-of-sky geometry has a smaller and opposite effect on comet detections in C3. The maximum heliocentric distance at which comets leave C3 varies from 3.5 $R_\odot$ to 8.5 $R_\odot$ throughout the year, meaning the peak brightness is always within the C3 field of view. However, the signal to noise and vignetting are worse closer to the occulting disk, so there is a preference for geometries in which the comet peaks at a larger elongation. Thus, the detection rate is slightly higher from January to March and July to September, when the apparent heliocentric distance of the peak in the light curve is largest. Only the very brightest comets are seen near the outer edges of C3, so the varying distance at which comets enter the field of view does not affect the discovery rate.

6.1.3. Phase Angle

Another effect of the geometry is the changing phase angle at which *SOHO* observes the comets at a given heliocentric distance (Figure 16). Comets which reach perihelion from September to January have phase angles greater than 100° for most or all of the time they are within the C3 field of

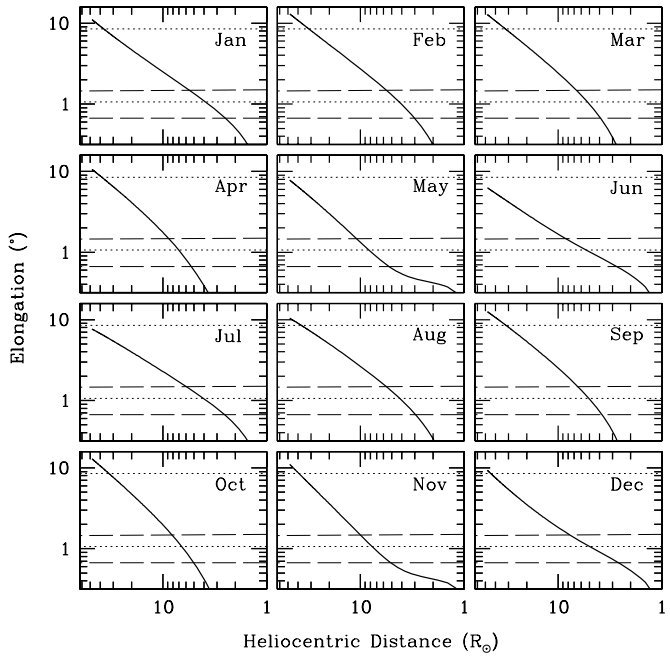

Figure 15. Solar elongation as a function of heliocentric distance for typical Kreutz comets. The track is for a comet which reaches perihelion on the 15th day of the month specified in each plot. The heavy line is the last three days of the orbit prior to perihelion. The post-perihelion track is not plotted since no Kreutz comets have been seen by *SOHO* after perihelion. The dotted and dashed horizontal lines denote the outer (upper) and inner (lower) radii of the C3 and C2 coronagraphs, respectively.

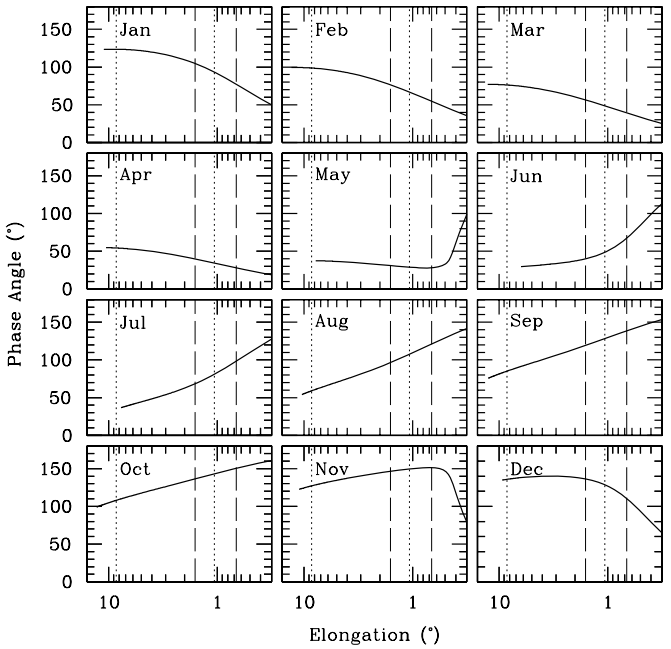

Figure 16. Monthly phase angle as a function of elongation for typical Kreutz comets. The track is for a comet which reaches perihelion on the 15th day of the month specified in each plot. The heavy line is the phase angle of the last three days prior to perihelion. The post-perihelion track is not plotted since no Kreutz comets have been seen by *SOHO* after perihelion. The dotted and dashed vertical lines denote the outer (left) and inner (right) radii of the C3 and C2 coronagraphs, respectively.

view. Forward scattering causes these comets to appear brighter than identical comets which reach perihelion from February to August, when they are at moderate phase (30°–100°). Thus, C3-detection rates are enhanced from September to January. Similarly, C2-detection rates are enhanced from August to December when comets are forward scattering in the C2 field of view.

6.1.4. SOHO*-centric Distance*

A final effect of the geometry is that the comets are closer to the spacecraft from September to March than they are from April to August. At the extremes, comets which reach perihelion in November and December (when approaching from the near side of the Sun) are ∼10% closer than comets which reach perihelion in May and June (when approaching from the far side of the Sun). As a result, a comet which arrives in November or December would appear ∼0.2 mag brighter than an identical comet which arrives in May or June. Thus, slightly more comets are detectable from September to March than from April to August.

6.2. True Arrival Rate

Over *SOHO*'s first 13 years, 1996–2008, 1354 Kreutz family comets were discovered in its images (Table 5). The discovery rate has increased throughout the mission due to a number of factors. First, the telemetry bandwidth allocated to C2 and C3 increased from 1996 to 2000, resulting in more full-resolution images per day. While an average of only six full-resolution images were taken per day by both C2 and C3 in 1996, the rate had increased to about 60 per day in C2 and 40 per day in C3 by 2000, and has remained relatively constant ever since. Increasing the image cadence allows fainter comets to be discovered because the time necessary for the comet to remain above the detection threshold is shorter.

The duty cycle, or the fraction of time *SOHO* takes images, also increased from 1996 to 2000. Following the definition of Biesecker et al. (2002), we define a gap in excess of four hours between full-resolution images in a given telescope to be significant, with the time exceeding four hours considered to be lost time. All of the excess time is then summed for a whole year, divided by the total hours in a year, and subtracted from 1. A year with no missed time would have a duty cycle of 1.0, while a year with no full-resolution images would be defined to have a duty cycle of 0. Due to the lower bandwidth allocated to C2 and C3 early in the mission, as well as significant hardware failures endured by the spacecraft in 1998 and 1999, the duty cycle for both C2 and C3 has been higher since 2000.

The "Sungrazing Comets" Web site became commonly used as a means of reporting comet discoveries in late 2000.[21] This site allows amateur comet hunters to download images in near real time to search for new comets. Since mid-2000, virtually every Kreutz comet has been discovered in near real time. In addition to searching the real time images, many users have systematically combed the archives for earlier comets, and it is believed that very few Kreutz comets have escaped detection.

Beginning in mid-2003, *SOHO* has been rolled by 180° approximately every three months. The roll periods cause an increase in detections in C3 due to the rotation of the occulting arm out of the path of Kreutz comets. Furthermore, there is an increase in the telemetry devoted to C2 for a few days on either side of each roll maneuver which causes a slight increase in the C2-detection rate.

[21] Publicly available reporting of amateur discoveries began in late 2000; however, the *SOHO* team had been working privately with amateurs for several years prior to this.

Table 5
Yearly *SOHO* Kreutz Discoveries and Estimated Detection Biases from 1996 to 2008

Year	C2	C3	Total	Missed Due to Spacecraft Failure	Extra Due to Increased Cadence	Extra Due to Roll	Extra Due to Human Bias	Net	Duty Cycle	Corrected Number
1996	9	26	27	0	0	0	0	27.0	0.735	36.7
1997	55	31	69	0	0	0	0	69.0	0.946	72.9
1998	66	17	70	22	0	0	0	92.0	0.928[a]	99.1
1999	53	33	71	3	1.6	0	0	72.4	0.862[a]	84.0
2000	69	32	79	0	8.9	0	0	70.1	0.944	74.3
2001	77	32	84	0	9.7	0	0	74.3	0.944	78.7
2002	91	38	106	0	16.5	0	6.2	83.3	0.957	87.0
2003	98	65	131	0	12.7	0	4.2	114.1	0.917	124.4
2004	105	84	146	0	11.3	12.7	8.2	113.7	0.888	128.1
2005	117	86	145	0	19.0	10.7	5.2	110.0	0.964	114.2
2006	114	72	141	0	15.2	7.7	6.0	112.1	0.893	125.6
2007	125	80	150	0	15.2	5.7	6.0	123.1	0.920	133.9
2008	113	67	135	0	15.2	0.7	6.0	113.1	0.932	121.4

Notes. Column (1) is the year. Columns (2) and (3) are the number of comets seen in C2 and C3, respectively. Column (4) is the total number of comets seen, which is less than the sum of Columns (2) and (3) because many comets are seen in both telescopes. Column (5) is the estimated number of comets not discovered due to data gaps caused by spacecraft failure. Column (6) is the estimated number of comets that were discovered due to the higher image cadence than in 1996–1998. Column (7) is the estimated number of comets that were discovered due to the roll of the telescope. Column (8) is the estimated number of comets that were accepted as comets due to changing human bias. Column (9) is the net number of discoveries after adding the misses (Column (5)) and subtracting the increases (Columns (6)–(8)). Column (10) is the duty cycle. Column (11) is the number of detections after correcting the net number for the duty cycle.
[a] The duty cycles for 1998 and 1999 are the average duty cycles during the times when the telescope was operational (i.e., excluding the gaps due to spacecraft failure).

Taking all of the above factors into account, the period since 2004 has the most complete temporal coverage and the most uniform month-to-month selection effects. We use the five years 2004–2008, corrected for the duty cycle, as the true monthly discovery rate of *SOHO*. There is no reason to think the flux varies from month to month, so months with lower discovery rates likely have fewer detections because of selection effects. Since May had the most detections, on average, we estimate the actual flux of Kreutz comets to be the May flux (0.67 comets day^{-1} = 21 comets month^{-1} = 247 comets year^{-1}). This is significantly higher than the rate of 14 comets month^{-1} found by Bzowski & Królikowska (2005) using data from 1997 to 2002 and the lower limit of 60 comets year^{-1} found by Biesecker et al. (2002), but is reflective of the improved discovery circumstances and the apparent overall increase in comet flux since then (discussed in the following section).

This rate is still only a lower limit, as the spacecraft distance and phase angle effects are sub-optimal during May. In principle, these effects could combine to improve the detection threshold by another 0.7 mag (0.2 mag due to the spacecraft distance and 0.5 mag due to the phase angle). Since the size distribution of the Kreutz family heavily favors small comets, an ideal scenario where the viewing geometry and detector sensitivity are all aligned could yield ∼60% more comet detections, all at the small end of the size distribution.

6.3. Quantifying the Change in Comet Flux

While the number of Kreutz comets discovered by *SOHO* has increased since the beginning of the mission, we must correct for all of the changing detection biases before concluding that the flux has truly increased. The corrections discussed below are given in Table 5. First, we estimated the number of comets that were missed due to the significant spacecraft failures in 1998 and 1999. We estimated the number of missed detections for 1998 July–October as the average of the detection rates from 1997 to 1999 July–October, and for 1999 January as the average of the detection rate from 1998 to 2000 January.

We estimated the number of comets which were discovered due to a higher image cadence. From 1997 to 1998, an average of 42 C2 orange images and 25 C3 clear images were taken per day (the rates were lower in 1996 and most were not full resolution 1024 × 1024). We used this as a baseline and randomly removed images from the data set of the comets discovered from 1999 to 2005 at a rate proportional to the average excess number of images in a given telescope per day for that year. We created 10 simulated data sets and determined the numbers of comets observed at different magnitudes, the length of observation, and the number of images in which the comet was observed. This allowed us to estimate the number of comets which would not have been discovered during 1997–1998, either because they did not reach the brightness threshold or because they were not observed in enough images.

We estimated the number of comets which have been discovered due to the roll of the telescope (starting in mid-2003) which would not have been discovered prior to then. Since the raw number of comets discovered has increased as the mission has progressed, we took the ratio of the average number of detections from April to December in 2004–2008 relative to the average number of detections from April to December in 1999–2003 (we exclude 1996–1998 due to the lower image cadence). We then multiplied this ratio by the average number of detections from January to March in 1999–2003, to estimate the number of comets we would have expected in January to March 2004–2008 due to the baseline increase in detections. Finally, we subtracted the expected number from the actual

number detected to estimate the increase due to the telescope roll.

A final bias we attempted to correct for was the human element. In our calculation of the photometry of more than 900 comets, it subjectively appears that more comets of dubious quality have been discovered as the mission has progressed. This could be due to either changes in the *SOHO* team members confirming comet discoveries and reporting them to the IAU or an improvement in the ability of the amateurs discovering comets. Doug Biesecker was the primary *SOHO* team member who verified comet discoveries and reported them to the IAU through mid-2002. Derek Hammer, whose involvement with the project dated back to 2000, replaced Biesecker in mid-2002 and continued in that role until mid-2003. Karl Battams has held the position since early 2004. The difference in personal bias in what constitutes a comet discovery could result in an increase in questionable comets. However, the number of *SOHO* "X-comets,"[22] objects which show properties consistent with being a comet but lack sufficient evidence for a confirmation, has remained relatively constant at ∼5 comets year^{-1}. This suggests that the threshold for accepting an object as a comet has remained relatively constant throughout the mission, independent of the individual making the confirmations. The amateurs discovering comets have unquestionably become more skilled at picking faint comets out of the noise. It is unclear how thoroughly the archival data have been searched at these levels, and the increase in dubious detections may simply reflect that the data have been searched more thoroughly in recent years.

Regardless of the cause, the number of comets whose brightest raw magnitude was fainter than 8 increased sharply during 2002–2003 and has remained high since. To quantify the increase, we averaged the number of comets year^{-1} fainter than magnitude 8 discovered from 1997 to 2001 (again ignoring 1996 due to its poor discovery circumstances). This was multiplied by the ratio of the number of comets brighter than magnitude 8, discovered from 2002 to 2005 relative to 1997–2001, to estimate the number of comets fainter than magnitude 8 that would be expected in 2002–2005 based on the overall increase in comet detections. Finally, we subtracted the expected number from the actual number of observed comets fainter than magnitude 8 from 2002 to 2005 to yield an estimate of the human bias.

Combining all of these effects and dividing by the average combined C2 and C3 duty cycle for each year, we estimated the normalized number of detections for each year. We included estimates for 2006–2008 (years for which we have not yet calculated photometry), where the increase due to the cadence was the average from 2004 to 2005, the increase due to the roll was calculated in the manner discussed above, and the increase due to human bias was the average from 2002 to 2005. From 1997 to 2002 a corrected average of 83.5 ± 8.4 comets year^{-1} were discovered, while from 2003 to 2008 124.6 ± 6.6 comets year^{-1} were discovered. Even after correcting for the varying circumstances throughout the mission, the increase in discoveries remains evident.

The jump in discoveries is not restricted to the faintest comets. The number of comets year^{-1} brighter than magnitude 6 rose from an average of 18.1 ± 3.1 from 1997 to 2002 to 32.6 ± 4.9 from 2003 to 2005, an increase of 80%. Comets magnitude 6 and brighter are typically observed for at least 24 hr and should have been easily discovered throughout the mission. Therefore, the changing discovery circumstances have little to no effect on the rate of discovery of these comets.

Sekanina & Chodas (2007) noted the increase in raw discoveries, and suggested it may be "an early warning of another cluster of bright sungrazers approaching the Sun in coming decades." Our much more rigorous analysis of the detection statistics supports this finding. Coupled with the appearance in mid-2002 of comets with a rather intermediate light curve shape and peak distance (Section 4.1), their suggestion of "a nonuniform distribution of mini-comets along the filament" is plausible.

Could the increasing flux explain the existence of the largest fragments with the currently observed size distribution? In order to explain the largest comets seen from the ground, the number of comets year^{-1} would have to increase by a factor of 26. If the increase seen from 1997 to 2008 is sustained, it would require ∼80 years of geometric increase or ∼750 years of linear increase to reach the necessary flux of comets. Given that the Kreutz orbital periods are 500–1000 years, the largest fragments are only consistent with the geometric increase scenario (since the linear increase would need ∼1500 years before the average flux was large enough). If all Kreutz comets are part of a continuous size distribution, then we must currently be at or near the minimum flux.

6.4. Comparison with Previous Space-based Coronagraphs

Nineteen Kreutz comets were discovered in *SMM* and *Solwind* images from 1979 to 1989, while *Skylab* observed for nine months in 1973–1974 without discovering any comets. The fields of view of *Skylab* (1.9–6 $R_\odot$), *Solwind* (2.5–10 $R_\odot$), and *SMM* (1.6 $R_\odot$ to between 4.8 $R_\odot$ and 6.5 $R_\odot$) were smaller than *SOHO* (Hundhausen et al. 1984; Howard et al. 1985), and the detectors were less sensitive. The estimated limiting magnitude was 6 for *SMM* (MacQueen & St. Cyr 1991). *Skylab* had "very similar capabilities [to *SMM*] for detection of coronal features" (Hundhausen et al. 1984). The limiting magnitude of *Solwind* was likely ∼4 (discussed further below). Can these differences explain the much lower detection rate relative to *SOHO*, or is this further evidence of a nonuniform distribution of small comets around the orbit?

To compare the discovery rates of *Skylab*, *Solwind*, and *SMM* with the discovery rate of *SOHO*, we considered all comets which were seen by *SOHO* from 1996 to 2005 at elongations within the fields of view of *Skylab*, *Solwind*, and *SMM*. Because the *SMM* detectors were aligned in a diamond pattern with the Sun at the center and the cardinal directions at the vertices, the field of view varies substantially by position angle. We considered both the maximum and minimum elongations of *SMM* separately. We then determined the brightest point for the comet within each field of view, adding 1 mag to all orange magnitudes to correct for the orange–clear color difference. We took the total number of comets seen by *SOHO* brighter than a particular magnitude in the appropriate field of view (*Skylab*, *Solwind*, or *SMM*), divided by the effective observing time of *SOHO* (8.68 years), then multiplied by the effective observing time of the telescope. This yielded the number of comets we would expect *Skylab*, *Solwind*, or *SMM* to have seen if the size distribution of Kreutz comets reaching perihelion was the same as from 1996 to 2005. We additionally calculated the likelihood that a particular number of comets of a given brightness would be seen by assuming the distribution was randomly distributed throughout the Kreutz orbit at the rate seen by *SOHO*, and simulating the observing interval 10,000 times.

[22] http://sungrazer.nrl.navy.mil/index.php?p=xcomets.

6.4.1. Skylab *(1973–1974)*

The *Skylab* coronagraph operated for 227 days, with an effective observing time of 93 days when a minimum of one observation per orbit was required for the duty cycle (Hundhausen et al. 1984). If we assume the limiting magnitude was 6 (as with *SMM*), then 1.1 comets would have been expected to be observed, with a 33% chance of observing none. If instead the limiting magnitude was 4, we would have expected 0.4 comets to be observed, with a 71% chance of observing none. Considering the short effective observation time and that the arrival times of Kreutz comets tend to be clustered (e.g., Marsden 1989; MacQueen & St. Cyr 1991), the non-detection of comets in the *Skylab* data set is not inconsistent with the *SOHO*-observed size distribution.

6.4.2. Solwind *(1979–1985)*

Solwind observed from 1979 March until 1985 September. We calculated the equivalent observing time in a similar fashion as the duty cycle calculation for *SOHO*, assuming that any gap in excess of 3 hr (the typical duration of *Solwind* comet observations) was lost time. This yielded a total equivalent observing time of 4.4 years, somewhat higher than the equivalent observing time (3.6 years) that would be derived by using the duty cycle of 54.9% calculated by Howard et al. (1985) from 1979 to 1981 and applying it to the whole mission.

We use the magnitudes estimated on the discovery IAU circulars and those calculated by Rainer Kracht,[23] yielding (in descending order of brightness): −4, −3, −2.5, −1.5,[24] −0.8, 0.5, 2.5, 2.5, and 3.0 for the nine Kreutz comets observed by *Solwind*. Kracht, an expert comet hunter who has found more than 200 comets in coronagraphic images, methodically searched the *Solwind* images[25] and found four comets which had not been discovered during the mission (Kracht & Marsden 2005a, 2005b, 2005c). R. Kracht reports that the faintest stars he could identify in *Solwind* images were magnitude 4.3–4.5 (2008, private communication). Thus, we conservatively take the limiting magnitude to be 4.

Using the rate seen by *SOHO*, we would expect 14.7 comets magnitude 4 or brighter in the 4.4 years of equivalent observing for *Solwind* (nine were found), 2.6 comets magnitude 2 or brighter (six were found), and 0.5 comets magnitude 0 or brighter (five, and possibly six considering the large uncertainties in brightness, were found). The total number of comets observed by *Solwind* is consistent with the *SOHO* distribution for comets magnitude 4 and brighter (23% chance of seeing nine or fewer comets magnitude 4 or brighter), however there were more bright comets than expected (2.0% chance of seeing six or comets magnitude 2 or brighter and 0.01% chance of seeing five or more comets magnitude 0 or brighter).

6.4.3. SMM *(1979, 1984–1989)*

MacQueen & St. Cyr (1991) reviewed the 11 comets observed by *SMM* (10 discovered by *SMM* and one discovered by *Solwind*). All of these comets were observed at distances smaller than 10 $R_\odot$, most were observed for only ∼2 hr, and all were in six or fewer images. The light curves were flat or slightly increasing, the same phenomenon seen for the occasional comets observed at these distances in *SOHO* images.

We calculated the equivalent time that *SMM* was observing from 1980 to 1989 in a similar fashion as the duty cycle calculation for *SOHO*, assuming that any gap in white light images in excess of 2 hr (the typical duration of *SMM* comet observations) was lost time.[26] This yielded a total equivalent observing time of 4.6 yr for *SMM*. MacQueen & St. Cyr (1991) used slightly different methodology and found 4.4 years.

We used the apparent magnitudes published by MacQueen & St. Cyr (1991, in descending order of brightness: −2, −1, 0, +2, +2, +3, +3, +3, +5, +5, +6) as the peak magnitude for comparison with the *SOHO* rate. Using the smallest maximum elongation for the *SMM* detector and the equivalent observing time of 4.6 years, we would expect 12.2 comets magnitude 6 or brighter (11 were seen), 3.2 comets magnitude 3 or brighter (eight were seen), and 1.6 comets magnitude 1 or brighter (three were seen). There is a 29% chance that 11 or fewer comets would be seen of magnitude 6 or brighter, a 0.2% chance that eight or more comets of magnitude 3 or brighter would be seen, and a 14% chance that three or more magnitude 1 or brighter comets would be seen. Using the largest maximum elongation for the *SMM* detector, we would expect 25.4 comets magnitude 6 or brighter, 4.8 comets magnitude 3 or brighter, and 2.1 comets magnitude 1 or brighter. There is a 0.1% chance that 11 or fewer comets would be seen of magnitude 6 or brighter, a 1.4% chance that eight or more comets of magnitude 3 or brighter would be seen, and a 23% chance that three or more magnitude 1 or brighter comets would be seen. As with *Solwind*, there appears to be an excess of bright comets observed by *SMM*.

6.4.4. Combined Data Set

To create a more robust data set, we combined all the Kreutz comets discovered by space-based coronagraphs prior to *SOHO*. Taking a limiting magnitude for *Solwind* of 4 and using this as the threshold for detection by *Skylab*, *Solwind*, and *SMM*, 16 comets of the proper brightness were discovered. We combined the *SMM* and *Solwind* data sets and used 2 hr as the gap threshold throughout the missions. This avoids double counting the period in 1984–1985 when both telescopes were observing (the only comet discovered during this time was observed by both telescopes). Adding the 93 equivalent days that *Skylab* observed yields an equivalent observing time of 8.0 years for the three coronagraphs. We would expect 17.3 comets during this time from the *SOHO* rate (using the smaller maximum *SMM* field of view) with 16 or more occurring 69% of the time. If instead we take the limiting magnitude of all three telescopes to be 1, eight comets were seen while we would expect 3.2 comets with only a 1.5% chance of detecting eight or more. Thus, it appears that the total number of comets was about what would be expected based on the *SOHO* size distribution, however the number of bright comets was too high. Changing

[23] http://www.rkracht.de/solwind/index.htm.

[24] *Solwind* 5 = 1984 XII = C/1984 O2 was also observed by *SMM* and was estimated to be magnitude −1.0 by MacQueen & St. Cyr (1991). For the purposes of these calculations either estimate will suffice.

[25] http://lasco-www.nrl.navy.mil/solwind/fits/.

[26] Unlike *Solwind* and *SOHO*, *SMM* imaged the corona in four quadrants, with only one quadrant imaged at a time. Due to the geometry of the Kreutz orbit, comets were never seen in the "north" quadrant. Most were seen in the "west" and "south" quadrants, and a few in the "east" quadrant. Due to overlapping fields of view, some were seen in two quadrants. In calculating the duty cycle we ignored all "north" quadrant images, and required there to have been at least one "south," "east," and "west" image taken within 95 minutes (one orbit) of each other in order to consider each image for the duty cycle. A more rigorous determination of the duty cycle could account for the seasonal appearance of Kreutz comets in the quadrants. Removal of quadrants at the times when the Kreutz orbit cannot be seen in them would raise the equivalent observing time slightly but would not significantly affect the results.

the gap threshold, using the published duty cycles, or using the larger maximum *SMM* field of view produce only small changes to the equivalent observing time and expected number, and do not affect the conclusions.

6.4.5. Discussion

The arguments above suggest that the distribution of *SMM* and *Solwind* comets differed from the distribution of *SOHO* comets. There was an overabundance of bright comets in both samples, although the total number of comets detected was reasonable. The baseline of observations for *Skylab* was too short to conclude that the distribution was different from the *SOHO* distribution. Before drawing any conclusions regarding the distributions of these comets, we must first consider a number of assumptions made in these estimates.

Perhaps the most obvious concern is that the magnitudes of the comets and the limiting magnitudes of the telescopes have been estimated incorrectly. Stars of magnitude 6 can be seen in *SMM* images and are very similar in brightness to *SMM*-3 (1988 X = 1988l = C/1988 M1), whose brightness was estimated at magnitude 6. This comet was easy to see in a compressed JPG image, and it is doubtful that a significant number of comets this bright or brighter could have been missed (and certainly not more than 80% of them!). We feel it is unlikely that there is a substantial error in the magnitude to which the *Solwind* and *SMM* have been searched completely, as both have been search methodically by Rainer Kracht (2008, private communication). For the *Solwind* and *SMM* comets to be consistent with the *SOHO* distribution, the brightness estimates of the brightest comets would need to be revised downward significantly while the fainter comets remained unchanged in brightness.

Comparing the images of the first six *Solwind*-discovered comets (the faintest of which was estimated to be magnitude 0.5) with the latter four discovered comets (the brightest of which was magnitude 1.5), the brighter comets are very obvious at a glance in the images, while the fainter comets are barely visible. Furthermore, the brightest six all have long, distinct tails while the four fainter comets have short, indistinct tails. In general, the presence and length of a tail in *SOHO* images are correlated with the brightness of the comet, and serve as additional confirmation that the brightest *Solwind* comets are distinctly brighter than the faintest *Solwind* comets. Considering the relative brightnesses of individual comets and the estimated uncertainty in brightness of ± 0.5 mag for *SMM* (MacQueen & St. Cyr 1991, and likely similar for *Solwind*), the magnitude estimates seem reasonable.

Even if the limiting magnitudes of *SMM* and *Solwind* have been estimated correctly, it is possible that there are comets above the threshold which have been missed in the images because they were not seen in enough images. This is more likely for *SMM* with its smaller field of view; typical comets were seen in two or three images spanning $\sim$2 hr. Due to the apparently chaotic nature of the Kreutz light curve at small heliocentric distances, a comet near the magnitude limit might be detectable in one image but not in the preceding or subsequent images. This is more problematic for faint comets, as bright ones will likely stay above the threshold despite fluctuations in brightness. Furthermore, the brighter ones are more likely to have a visible tail, making them recognizable even if they are only observed in a single image. While comets were discovered in *SMM* and *Solwind* images with as few as two images, at least three images would be necessary to confirm that a faint comet lacking a tail is not a cosmic ray. Therefore, *SMM* and *Solwind* are likely incomplete near their limiting magnitudes.

Unfortunately, there are a number of factors which limit the appropriateness of comparing the *Solwind* and *SMM* comet magnitudes with the *SOHO* comet magnitudes. First, the bandpasses of the *Solwind* (4100–6350 Å) and *SMM* (5000–5350 Å) filters are different from either the *SOHO* orange (5400–6400 Å) or clear filter (4000–8500 Å). As discussed in Section 4.3, emission within a given bandpass will affect the magnitude estimate differently depending on the width of the bandpass. The *SMM* bandpass does not include the known bright sodium doublet (5890 and 5896 Å) which is included in the other three. It is likely that the *Solwind* magnitudes would fall between the *SOHO* orange and clear magnitudes due to the widths of the bandpasses relative to the strong sodium emission while the *SMM* magnitude would be larger (fainter) than the *SOHO* clear magnitude due to the lack of the sodium emission line. This is consistent with the estimated magnitudes, as the *Solwind* comets were reported to be significantly brighter than the *SMM* comets, and the one comet seen by both (*Solwind* 5 = 1984 XII = C/1984 O2) was estimated to be 0.5 mag brighter in *Solwind*. Our estimates of the number of comets which should have been seen in *SMM* and *Solwind* images were dependent on the magnitude limits being on the same scale as the *SOHO* clear filter. Thus, for direct comparison with the *SOHO* discovery rates, it is likely that the limiting magnitude of *SMM* was overestimated (it could not see comets as faint as claimed) while the limiting magnitude of *Solwind* was underestimated (it could see comets fainter than claimed).

Second, no phase angle correction has been made. Phase corrections for both *SMM* and *Solwind* range from approximately -0.1 mag (the comet would have appeared slightly brighter at 90° phase) to +2 mag (the comet would have appeared much fainter at 90° phase).[27] Phase corrections do not meaningfully alter the distribution of detections. They do make several of the brightest comets fainter, but not by enough to make the rate of bright comets observed by either telescope agree with the *SOHO* rate.

Next, no attempt has been made to correct the discovery rate for the vignetting of any of the telescopes. While this is likely to have a seasonal effect on the detection rate, it is unlikely to prevent the detection of the extremely bright comets, and should have little effect on the rate estimate. The magnitudes have not been normalized to unit spacecraft-centric distance, however there is typically less than a 3% difference from 1 AU, making a negligible difference in the magnitude estimates. Finally, there is the inherent uncertainty of the comet position, estimated at $\pm 0.1\ R_\odot$ for *SMM* (MacQueen & St. Cyr 1991), and likely similar for the *Solwind* comets. This uncertainty has a minimal effect on the magnitude estimate and can safely be ignored.

Changing these assumptions does not substantially alter the conclusion that the *SMM* and *Solwind* comets have a different size distribution or frequency of arrival than the *SOHO* comets. However, there are myriad differences between *Solwind*, *SMM*, and *SOHO* data sets and the likelihood that the *Solwind* and *SMM* data sets are not complete at fainter magnitudes. While the distributions appear to be different, we cannot say so with certainty, and explore possible interpretations in the following section.

[27] It is difficult to estimate the phase correction for many of the *SMM* comets as the ephemeris generated by Horizons (http://ssd.jpl.nasa.gov/?horizons) differs substantially from some of the positions in Figure 6 of MacQueen & St. Cyr (1991), and the times of images given in some of the IAU circulars announcing the discoveries differ from those given on the image at the *SMM* C/P data archive (http://smm.hao.ucar.edu/smm/smmcp_cme.html).

6.4.6. Interpretation

There are several possible interpretations of the apparent higher rate of bright (i.e., large) comets reaching perihelion from 1979 to 1989 relative to 1996–2005. If we assume that the data were complete down to the estimated limiting magnitudes, then there were more large comets and fewer small comets (the size distribution was flatter) in the 1980s. In this case, the size distribution was different from that seen by *SOHO*, and the distribution of "debris" (small comets) around the Kreutz orbit evidently changes on timescales as short as 10–15 years. This could be indicative of a different fragmentation process or possibly be evidence for constituents of the progenitor nucleus having accreted in different parts of the solar nebula, where the size distribution in each area was different.

Alternatively, if we assume that the *SMM* and *Solwind* discoveries are incomplete at fainter magnitudes but had the same size distribution as the *SOHO* comets, then there were far more comets arriving in the 1980s than since 1996, with a tremendous population of comets fainter than magnitude 3–4 going undetected. Looking at the *Solwind* and *SMM* data separately, there were more bright comets arriving from 1979 to 1984 than from 1984 to 1989, although the sample size is extremely small. Combined with the apparent increase in flux of *SOHO* comets beginning in 2003, this implies that the flux of comets varies around the orbit, and was in a local minimum during the 1990s. Since the most recent large, ground-observed comets arrived from 1963 to 1970 this may mean that the *Solwind* and *SMM* comets were the end of the distribution of fragments scattered from these large comets. In this scenario, the increasing flux of *SOHO* comets since 1996 presages a major fragment which will arrive in the next few decades. Since the majority of *SOHO* comets are subgroup I objects (with the caveat that most *SOHO*-derived orbits are not well determined), the coming major fragment is likely to be of subgroup I.

A final interpretation is that the discoveries are relatively complete to the nominal limiting magnitudes, but because the light curves of individual comets are chaotic at distances smaller than 6–8 $R_\odot$, the magnitudes of the comets seen by *SMM* and *Solwind* do not correspond to their sizes. As a result, small comets may appear brighter (i.e., bigger), and we can only compare the overall rate of discovery and not the relative rate of bright versus faint comets. Then the *Skylab*, *Solwind*, and *SMM* discovery rates are consistent with those of *SOHO*, and there has been minimal change in the flux of Kreutz comets reaching perihelion since at least 1979 (with the exception of the increase from 2002 to 2003 discussed above). However, a comparison of all *SOHO* comets which were observed from 10 to 15 $R_\odot$ and at less than 8 $R_\odot$ (226 comets) reveals very good correlation between the magnitudes at both distances. Despite the chaotic nature of the light curves inside 8 $R_\odot$, comets that are brighter from 10 to 15 $R_\odot$ are also brighter inside 8 $R_\odot$. Therefore, it is likely that the *SMM* and *Solwind* magnitudes do correspond to their sizes, and this interpretation is invalid.

7. THE FUTURE OF KREUTZ OBSERVATIONS

7.1. STEREO

Although *SOHO* continues to operate, the next advance in space-based coronagraphs, *STEREO*, is already in operation. *STEREO* observes the Sun in 3-D with two identical spacecraft. One spacecraft orbits ahead (*STEREO*-A) and the other trails the Earth (*STEREO*-B). Each spacecraft has two coronagraphs (COR1 and COR2) and two heliospheric imagers (HI1 and HI2). COR1 has an annular field of view from 1.3 to 4.0 $R_\odot$ with a resolution of 7.5 arcsec pixel^{-1}, and a bandpass of 6500–6600 Å. COR2 has an annular field of view from 2 to 15 $R_\odot$ with a resolution of 15 arcsec pixel^{-1} and a bandpass of 6500–7500 Å. HI1 is centered 13.°28 from the Sun with a square field of view 20° wide, a resolution of 70 arcsec pixel^{-1}, and a bandpass of 6500–7500 Å. HI2 is centered 53.°36 from the Sun with a square field of view 70° wide, a resolution of 240 arcsec pixel^{-1}, and a bandpass of 4000–10,000 Å. The heliospheric imagers on *STEREO*-A look back at the Earth–Sun line, while the heliospheric imagers on *STEREO*-B look ahead at the Earth–Sun line (Kaiser 2005; Howard et al. 2008).

STEREO's bandpasses, imaging sequences, and processing techniques are not as favorable for discovering comets as those of *SOHO*. However, it has observed more than 100 Kreutz comets which were seen by *SOHO* (e.g., Marsden & Battams 2008a, 2008b; Marsden et al. 2008) and has discovered more than a dozen Kreutz comets which were apparently unobserved by *SOHO* (Battams et al. 2008). *STEREO* cannot rival *SOHO* in sheer quantity of sungrazer detections, but the multiple vantage points provided by combining *STEREO*-A, *STEREO*-B, and/or *SOHO* data allow parallactic determination of orbits, resulting in much greater certainty. Furthermore, *STEREO*'s larger field of view should help understand the light curve behavior of Kreutz comets at distances larger than 30 $R_\odot$. Observations at these distances are likely to reveal a sharp increase in brightness from $\sim r^{-4}$ to $\sim r^{-7}$, and the heliocentric distance of this increase will give insight into the mechanism which causes it.

The stereoscopic viewing capabilities have already been used to derive the position of the comet's tail in three dimensions using direct triangulation (Thompson 2009). This analysis revealed that the particles making up the tail were released 18–24 hr before perihelion (18–22 $R_\odot$) and confirmed that the tail shape can be characterized by a synchrone with no motion out of the plane, as suggested by Sekanina (2000b) using low-resolution *SOHO* images. Investigation of other well-observed tails may demonstrate a link between the formation of a tail and the abrupt change in brightening slope seen between 20 and 30 $R_\odot$, and may improve estimates of the size of the dust particles in the tail.

Multiple viewing geometries will also allow a direct calculation of the scattering phase dependence by comparing the apparent magnitude of a comet as seen by each spacecraft. Understanding the dependence of scattering on the phase angle will allow estimates of the sizes of typical particles in the coma and of the dust-to-gas ratio of the coma. This will also improve the correction of the apparent magnitudes in the *SOHO* field of view, since the comets (Marcus 2007b) used to calculate the phase dependence were observed at much larger heliocentric distances and may have had different compositions, dust size distributions, and dust-to-gas ratios than do sungrazing comets.

7.2. Ground-based Telescopes

In the next few years, large-scale ground-based surveys such as Pan-STARRS (Hawaii) and LSST (Chile) are scheduled to begin collecting data. With the increase of survey telescopes largely dedicated to searching for comets and near-Earth objects, what are the chances that Kreutz comets will be observed from the ground?

A survey for Kreutz comets would look for them several months prior to perihelion. Due to the range of orbits, it is necessary to survey a wide area (at least 10 deg^2), ideally with non-sidereal tracking at the expected rate of motion of the

comets in that field of view. Because the comets are not known prior to being seen by *SOHO*, regions of the sky statistically likely to contain them must be chosen. The survey would ideally be carried out in the southern hemisphere with a telescope capable of imaging at relatively small solar elongations. Most surveys observe too far from the Sun to discover Kreutz comets, although Pan-STARRS has plans to look for near-Earth objects at "sweet spots" some 60° from the Sun along the ecliptic which may be successful.

The magnitude of the Kreutz comets at these distances is unknown, but the rate of brightening is likely steeper than $\propto r^{-3.5}$. Even if the slope of the brightening is much steeper than this, the flux of Kreutz comets is large enough that the occasional large (∼30 m) comet may be detected. If such a comet were bright enough, high time-resolution photometry might allow determination of the rotation rate and size, placing constraints on its internal composition. Discovery of a comet prior to its entering the *SOHO* field of view would allow the *SOHO* team to plan observing sequences such as cycling through the range of filters available on C2 and C3 (ideally with a higher cadence and shorter observing times since the brightest comets saturate the detector) and alignment of the UVCS spectrograph, all of which could give insight into the composition.

8. SUMMARY

This work has investigated the light curves of 924 Kreutz comets seen by *SOHO* from 1996 to 2005. While the information available from a single light curve is often minimal, studying them collectively has allowed us to draw conclusions about the Kreutz group as a whole. The Kreutz comets observed by *SOHO* have a power-law size distribution and they have a continuum of slightly different compositions. The individual light curves follow a similar shape, but differ due to each comet's unique composition and history. The distribution of these small comets may not be uniform around the orbit. We summarize the key results below.

1. The light curves do not have a bimodal distance of peak brightness as previously reported by Biesecker et al. (2002). Instead, they reach a peak in brightness over a range from 10.5 $R_\odot$ to 14 $R_\odot$ with a maximum around 12 $R_\odot$. This suggests that there is a continuum of compositions among the members rather than two distinct compositions.
2. Most light curves brighten near $\propto r^{-7.3}$ when they first become visible, exhibit a change in brightening rate between 20 $R_\odot$ and 30 $R_\odot$, then brighten near $\propto r^{-3.8}$ from 16 $R_\odot$ to 24 $R_\odot$. It is unclear how far outward the $\propto r^{-7.3}$ extends. The rate of brightening from 16 $R_\odot$ to 24 $R_\odot$ is similar to the rates of fading of the ground-observed members of the family as well as the canonical rate of brightening for most comets.
3. The comets appear brighter in the C2 and C3 orange filters than the C3 clear filter by ∼1 mag, although the difference varies with heliocentric distance, reaching a maximum near 19 $R_\odot$. We concur with previous authors (e.g., Biesecker et al. 2002; Sekanina 2003) that this difference in brightness is due to sodium emission.
4. The size range is 2–50 m in radius, but may be a factor of 2 larger or smaller due to a number of simplifying assumptions. The cumulative size distribution is $N(>R) \propto R^{-2.2}$. The largest fragment in this distribution should be ∼500 m in radius, consistent with the two smallest ground-observed Kreutz comets being the two largest members of the group. Six other ground-observed comets were much larger than this. If the distribution of comets seen by *SOHO* is consistent throughout an 800 year orbit, there are ∼20,000 comets larger than 5 m, having a total mass of $\sim 4 \times 10^{14}$ g. This is much smaller than the likely mass of the largest ground-observed members. From these arguments we conclude that either the size distribution does not extend to the largest sizes, or that the distribution is not uniform around the orbit.
5. The flux of Kreutz comets reaching perihelion has increased during the mission. After correcting for the changing discovery circumstances, the average comets year^{-1} increased from 83.5 ± 8.4 from 1997–2002 to 124.6 ± 6.6 from 2003–2008. The increase is not due to improved detection capabilities, as there was an 80% increase in comets brighter than magnitude 6. This suggests the increase is due to a changing distribution around the orbit.
6. There were more bright (large) comets observed with *Solwind* and *SMM* from 1979 to 1989 than would be expected from the *SOHO* data. Depending on the completeness of these data sets at fainter magnitudes, this may be due to a flatter size distribution or a different flux of comets reaching perihelion.
7. While *SOHO* is operational, it will continue to dominate the discovery of Kreutz comets. However, *STEREO* provides higher quality data over a larger range of distances for the comets it does observe. *STEREO* observations should help to understand the typical light curve at distances larger than 30 $R_\odot$ and should allow a more robust determination of scattering at large phase angles. Ground-based surveys may discover a small number of Kreutz comets. If recognized in a timely fashion, such discoveries would allow subsequent follow-up observation from the ground and special observing sequences by *SOHO* which may help constrain the size, rotation state, and composition.

Thanks to the anonymous referee for numerous suggestions that have improved the readability of the manuscript. We thank the members of the *SOHO* and *STEREO* teams who have helped at many stages of this work, especially Derek Hammer and Karl Battams, who have maintained the official sungrazer Web site since Doug Biesecker left. We also thank the many comet hunters who have made it possible to study nearly an order of magnitude more comets in this work than any paper to date. In particular, we thank Rainer Kracht for his helpful insight over the years. This work was supported by NASA Planetary Atmospheres grants NAG513295 and NNG06GF29G.

REFERENCES

A'Hearn, M. F., et al. 2005, Science, 310, 258
Battams, K., Baldwin, K., & Marsden, B. G. 2008, IAU Circ., 8926, 1
Bemporad, A., Poletto, G., Raymond, J. C., Biesecker, D. A., Marsden, B., Lamy, P., Ko, Y.-K., & Uzzo, M. 2005, ApJ, 620, 523
Biesecker, D. A., Lamy, P., St. Cyr, O. C., Llebaria, A., & Howard, R. A. 2002, Icarus, 157, 323
Brueckner, G. E., et al. 1995, Sol. Phys., 162, 357
Bzowski, M., & Królikowska, M. 2005, A&A, 435, 723
Curtis, G. W., & The Sacramento Peak Observatory Staff., 1966, AJ, 71, 194
England, K. J. 2002, J. Br. Astron. Assoc., 112, 13
Evans, C., & McKim Malville, J. 1967, PASP, 79, 310
Fernández, J. A., Tancredi, G., Rickman, H., & Licandro, J. 1999, A&A, 352, 327
Fernández, Y. R., Lisse, C. M., Kelley, M. S., Dello Russo, N., Tokunaga, A. T., Woodward, C. E., & Wooden, D. H. 2007, Icarus, 191, 424
Gehrz, R. D., & Ney, E. P. 1992, Icarus, 100, 162

Groussin, O., et al. 2007, Icarus, 187, 16
Grynko, Y., Jockers, K., & Schwenn, R. 2004, A&A, 427, 755
Hasegawa, I. 1966, The Heavens, 47, 31 (in Japanese)
Hasegawa, I., & Nakano, S. 2001, PASJ, 53, 931
Howard, R. A., Sheeley, N. R., Jr., Michels, D. J., & Koomen, M. J. 1985, J. Geophys. Res., 90, 8173
Howard, R. A., et al. 2008, Space Sci. Rev., 136, 67
Hundhausen, A. J., Sawyer, C. B., House, L., Illing, R. M. E., & Wagner, W. J. 1984, J. Geophys. Res., 89, 2639
Iseli, M., Küppers, M., Benz, W., & Bochsler, P. 2002, Icarus, 155, 350
Kaiser, M. L. 2005, Adv. Space Res., 36, 1483
Kimura, H., Mann, I., Biesecker, D. A., & Jessberger, E. K. 2002, Icarus, 159, 529
Kirkwood, D. 1880, The Observatory, 3, 590
Knight, M. 2008, SOHO-C-LASCO-4-COMETIMAGES-V1.0, NASA Planetary Data System
Knight, M. 2009, SOHO-C-LASCO-5-KREUTZPHOTOM-V1.0, NASA Planetary Data System
Knight, M. M., Walsh, K. J., A'Hearn, M. F., Swaters, R. A., Zauderer, B. A., Samarasinha, N. H., Vázquez, R., & Reitsema, H. 2007, Icarus, 187, 199
Kolokolova, L., Hanner, M. S., Levasseur-Regourd, A.-C., & Gustafson, B. Å. S. 2004, in Comets II, ed. M. C. Festou, H. U. Keller, & H. A. Weaver (Tucson, AZ: Univ. of Arizona Press), 577
Kracht, R., & Marsden, B. G. 2005a, IAU Circ., 8566, 1
Kracht, R., & Marsden, B. G. 2005b, IAU Circ., 8583, 1
Kracht, R., & Marsden, B. G. 2005c, IAU Circ., 8573, 1
Kresák, L. 1966, Bull. Astron. Inst. Czech., 17, 188
Kreutz, H. 1888, Untersuchungen Über das Cometensystem 1843 I, 1880 I und 1882 II (Kiel: Druck von C. Schaidt, C. F. Mohr nachfl.)
Kreutz, H. 1891, Publication der Koeniglichen Sternwarte in Kiel, 6
Kreutz, H. 1901, Astron. Nachr., 155, 63
Lamy, P., Biesecker, D. A., & Groussin, O. 2003, Icarus, 163, 142
Lamy, P. L., Toth, I., Fernandez, Y. R., & Weaver, H. A. 2004, in Comets II, ed. M. C. Festou, H. U. Keller, & H. A. Weaver (Tucson, AZ: Univ. of Arizona Press), 223
Lisse, C. M., et al. 2006, Science, 313, 635
Llebaria, A., Lamy, P., & Danjard, J.-F. 2006, Icarus, 182, 281
Lowry, S., Fitzsimmons, A., Lamy, P., & Weissman, P. 2008, Kuiper Belt Objects in the Planetary Region: The Jupiter-Family Comets, 397
MacQueen, R. M., & St. Cyr, O. C. 1991, Icarus, 90, 96
Marcus, J. N. 2007a, IAU Circ., 8793, 2
Marcus, J. N. 2007b, Int. Comet Quart., 29, 39
Marcus, J. N. 2007c, Int. Comet Quart., 29, 119
Marcus, J. N., & Seargent, D. A. J. 1986, in ESA SP 250, ESLAB Symp. on the Exploration of Halley's Comet, Vol. 2: Dust and Nucleus,, 359
Marsden, B. G. 1967, AJ, 72, 1170
Marsden, B. G. 1989, AJ, 98, 2306
Marsden, B. G., & Battams, K. 2008a, Minor Planet Electron. Circ., F38
Marsden, B. G., & Battams, K. 2008b, Minor Planet Electron. Circ., G4
Marsden, B. G., Battams, K., & Baldwin, K. 2008, Minor Planet Electron. Circ., G15
Meech, K. J., Hainaut, O. R., & Marsden, B. G. 2004, Icarus, 170, 463
Michels, D. J., Sheeley, N. R., Howard, R. A., & Koomen, M. J. 1982, Science, 215, 1097
Morrill, J. S., et al. 2006, Sol. Phys., 233, 331
Ney, E. P. 1982, in IAU Colloq. 61, Comet Discoveries, Statistics, and Observational Selection, ed. L. L. Wilkening (Tucson, AZ: Univ. of Arizona Press), 323
Ney, E. P., & Merrill, K. M. 1976, Science, 194, 1051
Preston, G. W. 1967, ApJ, 147, 718
Raymond, J. C., et al. 1998, ApJ, 508, 410
Schulz, R., Owens, A., Rodriguez-Pascual, P. M., Lumb, D., Erd, C., & Stüwe, J. A. 2006, A&A, 448, L53
Sekanina, Z. 1967a, Bull. Astron. Inst. Czech., 18, 198
Sekanina, Z. 1967b, Bull. Astron. Inst. Czech., 18, 229
Sekanina, Z. 2000a, ApJ, 542, L147
Sekanina, Z. 2000b, ApJ, 545, L69
Sekanina, Z. 2002a, ApJ, 576, 1085
Sekanina, Z. 2002b, ApJ, 566, 577
Sekanina, Z. 2003, ApJ, 597, 1237
Sekanina, Z., & Chodas, P. W. 2002a, ApJ, 581, 760
Sekanina, Z., & Chodas, P. W. 2002b, ApJ, 581, 1389
Sekanina, Z., & Chodas, P. W. 2004, ApJ, 607, 620
Sekanina, Z., & Chodas, P. W. 2007, ApJ, 663, 657
Sekanina, Z., & Chodas, P. W. 2008, ApJ, 687, 1415
Sheeley, N. R., Jr., Howard, R. A., Koomen, M. J., & Michels, D. J. 1982, Nature, 300, 239
Slaughter, C. D. 1969, AJ, 74, 929
Snodgrass, C., Fitzsimmons, A., Hainaut, O., Hamuy, M., Hutsemekers, D., Jehin, E., Jones, M., & Manfroid, J. 2007, Cent. Bur. Electron. Tel., 832, 1
Spinrad, H., & Miner, E. D. 1968, ApJ, 153, 355
Strom, R. 2002, A&A, 387, L17
Sunshine, J. M., Groussin, O., Schultz, P. H., A'Hearn, M. F., Feaga, L. M., Farnham, T. L., & Klaasen, K. P. 2007, Icarus, 190, 284
Tancredi, G., Fernández, J. A., Rickman, H., & Licandro, J. 2006, Icarus, 182, 527
Thernisien, A. F., Morrill, J. S., Howard, R. A., & Wang, D. 2006, Sol. Phys., 233, 155
Thompson, W. T. 2009, Icarus, 200, 351
Uzzo, M., Raymond, J. C., Biesecker, D., Marsden, B., Wood, C., Ko, Y.-K., & Wu, R. 2001, ApJ, 558, 403
Watanabe, J.-i., Kawakita, H., Furusho, R., & Fujii, M. 2003, ApJ, 585, L159
Weaver, H. A., Lisse, C. M., Mutchler, M. J., Lamy, P., Toth, I., & Reach, W. T. 2006, BAAS, 38, 490
Weaver, H. A., et al. 2001, Science, 292, 1329
Weidenschilling, S. J. 2004, in Comets II, ed. M. C. Festou, H. U. Keller, & H. A. Weaver (Tucson, AZ: Univ. of Arizona Press), 97
Weissman, P. R. 1983, Icarus, 55, 448
Weissman, P. R., & Lowry, S. C. 2003, in Lunar and Planetary Institute Conference Abstracts, Vol. 34, ed. S. Mackwell & E. Stansbery